

# We are IntechOpen, the world's leading publisher of Open Access books Built by scientists, for scientists

6,900

Open access books available

186,000

International authors and editors

200M

Downloads

Our authors are among the

154

Countries delivered to

TOP 1%

most cited scientists

12.2%

Contributors from top 500 universities



WEB OF SCIENCE™

Selection of our books indexed in the Book Citation Index  
in Web of Science™ Core Collection (BKCI)

Interested in publishing with us?  
Contact [book.department@intechopen.com](mailto:book.department@intechopen.com)

Numbers displayed above are based on latest data collected.  
For more information visit [www.intechopen.com](http://www.intechopen.com)



# On the Possibility of Layered Crystals Application for Solid State Hydrogen Storages – InSe and GaSe Crystals

Yuriy Zhirko, Volodymyr Trachevsky and Zakhar Kovalyuk

Additional information is available at the end of the chapter

<http://dx.doi.org/10.5772/50307>

## 1. Introduction

Among the variety of chemical compounds that are available in nature, the class of layered crystals comprises a specific place. As can be seen in Fig. 1, it is rather wide and covers the range from simple compounds of the graphite type up to silicates, micas and organic compounds.

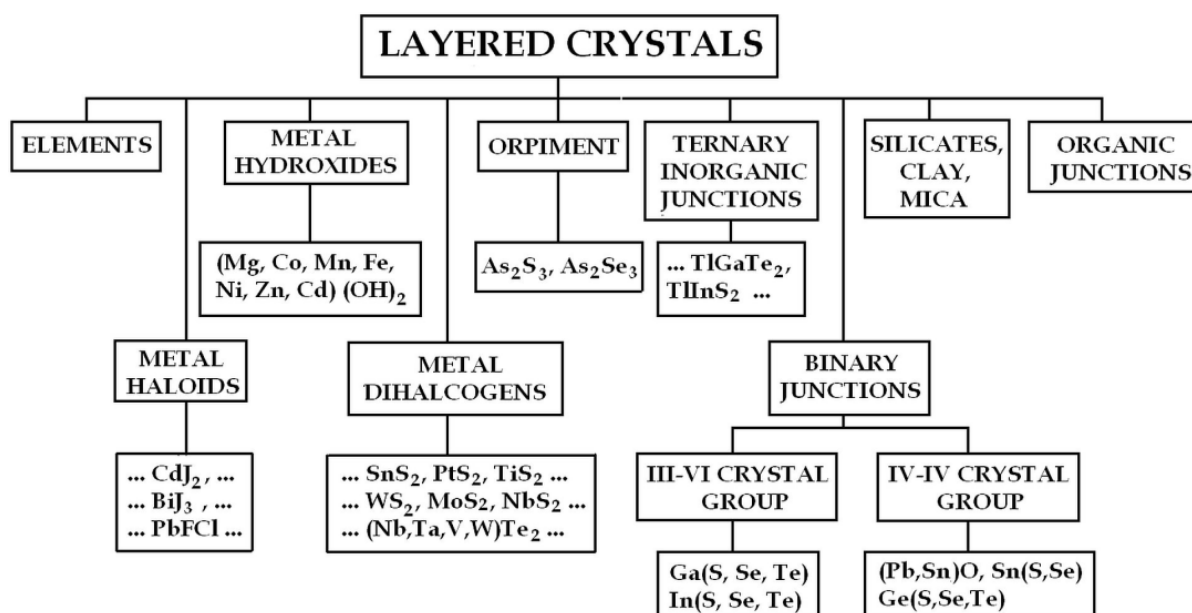


Figure 1. Class of layered crystals

Due to their natural properties, as a rule layered crystals easily dissolve in their bulk various molecular gases, beginning from hydrogen and methane up to complex organic molecules.

This circumstance makes them very attractive for application as solid-state hydrogen storages.

In this work, using the example of InSe and GaSe layered crystals and modern methods of scientific investigations, we have considered some aspects to deeper ascertain physical-and-chemical processes taking part during intercalation and deintercalation of layered crystals with hydrogen.

As is shown on a Fig.1 discussed in this work InSe and GaSe layered crystals are related to binary compounds  $A_3B_6$  where crystalline layers consist of four monolayers including Se and In(Ga) atoms and located one above another in the sequence Se-In(Ga)-In(Ga)-Se. These atoms are bound to each other by ion-covalent hybrid  $sp^2$ -bonds. Inside crystalline layers, orientation of atoms corresponds to the spatial group  $D_{3h}$ . In this case (see Fig. 2b), each In(Ga) atom inside crystalline layer yields its two valent electrons to three nearest Se atoms to fill their  $p$ -shells. The remaining electron of this In(Ga) atom together with the remaining electron of the adjacent In(Ga) atom in this layer form a filled  $s$ -shell. This causes configuration in which orbitals of valent electrons are located inside the layer and are not practically overlapped with orbitals of valent electrons related to atoms in the neighboring layer. As a result, the adjacent layers are only linked with a weak van der Waals bond.

This clearly pronounced anisotropy of chemical bonds between layers and inside crystalline layers allows intercalation of layered crystals, i.e. introduction of foreign atoms or molecules into the interlayer space of grown crystals. For example, in InSe and GaSe crystals the volume of the van der Waals space (the so-called "van der Waals gap") comprises 40...45 % of all the crystal bulk, while the internal surface of this space is close to  $(2...2.5) \cdot 10^3 \text{ m}^2$  per  $1 \text{ cm}^3$ .

It is known (Belenkii & Stopachinskii, 1983; Polian et al., 1976; Ghosh, 1983), that single crystals grown by the Bridgman method possess four polytypes ( $\beta$ -,  $\delta$ -,  $\varepsilon$ - and  $\gamma$ -) varying between each other in the sequence of crystalline layer stacking. As a rule (see Fig. 2a), InSe single crystals are of  $\gamma$ -polytype with rhombohedral (trigonal) crystalline structure (spatial group  $C_{3v}^5$ , in which the primitive unit cell contains one  $\text{In}_2\text{Se}_2$  molecule comprising three layers). The non-primitive hexagonal unit cell comprises three crystalline layers and consists of three  $\text{In}_2\text{Se}_2$  molecules, respectively. GaSe single crystals are of  $\varepsilon$ -polytype. These belong to hexagonal crystalline structure (spatial group  $D_{3h}^1$ ), the unit cell of which consists of two  $\text{Ga}_2\text{Se}_2$  molecules located within two crystalline layers.

Lattice parameters of the crystals  $\gamma$ -InSe and  $\varepsilon$ -GaSe are studied well. In the case of  $\varepsilon$ -GaSe, they are as follows: lattice parameters along the perpendicular to layers  $C_0 = 15.95 \text{ \AA}$  and in the layer plane  $a_0 = 3.755 \text{ \AA}$  (Kuhn et al., 1975). For  $\gamma$ -InSe, they are, respectively:  $C_0 = 25.32 \text{ \AA}$  and  $a_0 = 4.001 \text{ \AA}$ . The distances between the nearest atoms inside the layer (see Fig. 2c) are as follows:  $C_{\text{In-In}} = 2.79 \text{ \AA}$  and  $C_{\text{In-Se}} = 2.65 \text{ \AA}$ , respectively;  $\angle \varphi = 119.3^\circ$ , the layer thickness  $C_1 = 5.36 \text{ \AA}$ , the distance between layers  $C_i = 3.08 \text{ \AA}$ , while the distance between adjacent Se atoms located in different layers  $C_{\text{Se-Se}} = 3.80 \text{ \AA}$  (Goni et al., 1992; Olguin et al., 2003).

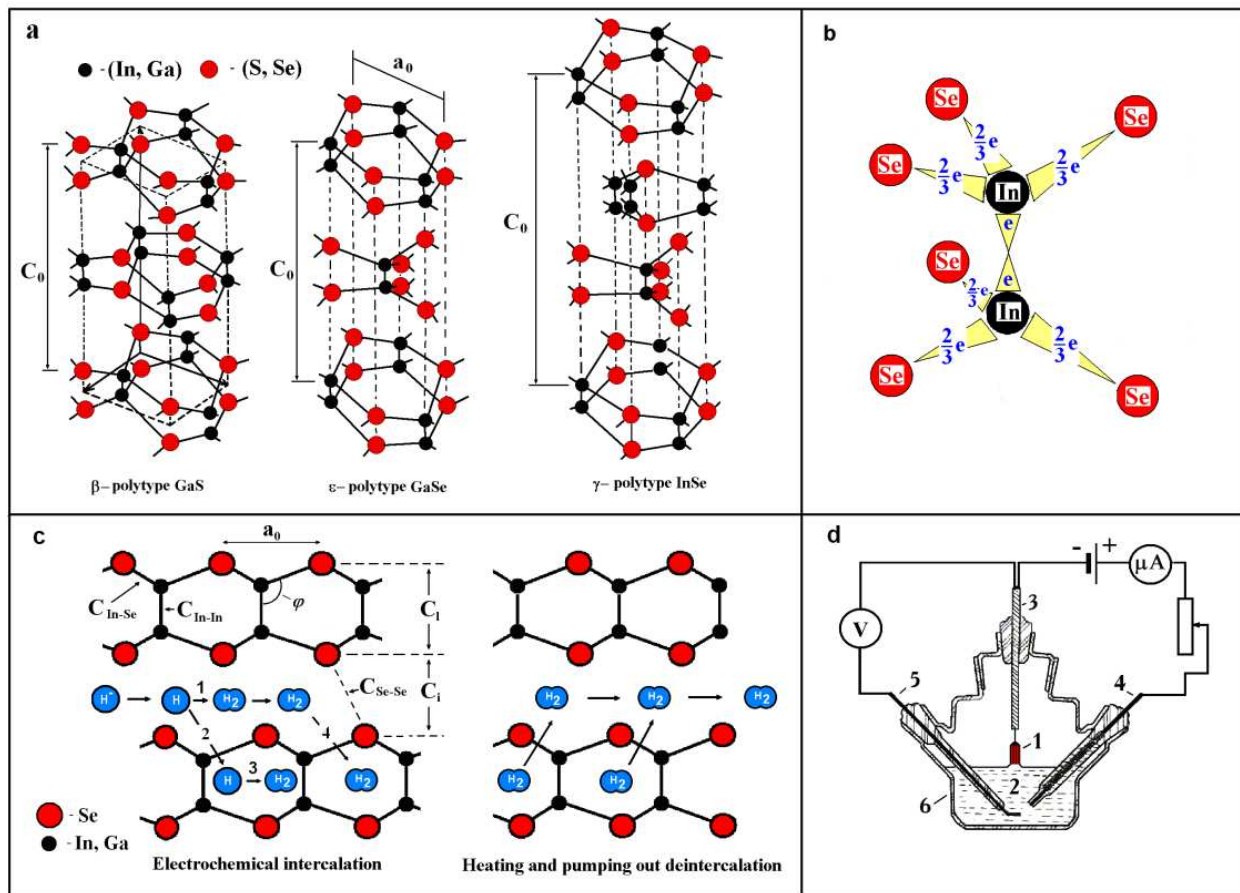


**Figure 2.** a – crystalline structure and layer stacking for various crystal polytypes of group; b – distribution of chemical bonds between atoms In(Ga) and Se inside the crystalline layer; c – two-dimensional scheme illustrating the intercalation and deintercalation processes for hydrogen in layered crystals InSe and GaSe; d – scheme of electrochemical cell: 1- layered crystal; 2 – electrolyte; 3 – operation platinum electrode; 4- comparative electrode (AgCl); 5 – auxiliary platinum electrode; 6 – cell body.

Undoubtedly, these unique properties of semiconductor compounds in this class, and in particular of InSe and GaSe crystals, attract special attention of researches, as heterostructures based on them possess good photosensitivity and can be used not only in solar elements (Martines-Pastor et al., 1987; Lebedev et al., 1998; Shigetomi & Ikari, 2000) and accumulators of electrical energy (Grigorochak et al., 2002), but in accord with investigations (Zhirko et al., 2012) are rather promising in creation of gamma radiation sensors.

Besides, as it was shown in a number of recent works (Kozmik et al., 1987; Zhirko et al., 2007a; Zhirko et al., 2007b), layered crystals InSe and GaSe can be applied in hydrogen energetics as operation elements in solid hydrogen storages. The hydrogen concentration in them can reach values close to  $x = 5...6$ , where  $x$  is the amount of embedded hydrogen atoms per one formular unit of the intercalated crystal matrix.

Described in this work is the method of hydrogen intercalation-deintercalation in InSe and GaSe crystals. Besides, being based on the performed complex electron-microscopic (SEM, EDS, HKL), radiospectroscopic (NMR, EPR), optical and electrophysical investigations, we

have discussed the model describing introduction of hydrogen into layered crystals InSe and GaSe as well as considered some physical aspects related to this process.

## 2. The method for hydrogen intercalation and deintercalation of InSe and GaSe layered crystals

Before the process of intercalation with hydrogen,  $\gamma$ -InSe and  $\varepsilon$ -GaSe bulk single crystals were used to spall crystalline plates along the cleavage planes with parallel mirror surfaces that do not require any further polishing or etching. To combine investigations of processes for hydrogen intercalation with those mentioned in Introduction, the sample thickness was chosen within the range 20 to 30  $\mu\text{m}$ , and linear dimensions were 5x5 mm. Powders with grain dimensions 5...20  $\mu\text{m}$  were prepared from  $\gamma$ -InSe and  $\varepsilon$ -GaSe single crystal ingots by using an ultrasound mill. For further investigations, these powders were pressed to tablets.

Intercalation with hydrogen was performed using the electrochemical method in the three-electrode glass cell made from chemically- and thermally-stable glass. The cell (see Fig. 2d) consisted of AgCl comparative electrode, operation and auxiliary (platinum wire) electrodes. The studied samples were sweated with wires on the operation electrode and placed into electrolyte consisting of 0.1 normal solution prepared from doubly distilled water and chemically-pure concentrated HCl acid.

Intercalation of the  $\gamma$ -InSe and  $\varepsilon$ -GaSe samples was performed using the way described in (Kozmik et al., 1987; Zhirko et al., 2007a) from electrolytic solution by the method of "pulling field" in the galvanostatic regime. The chosen special conditions for the optimal electric voltage and current density ( $E = 30...50 \text{ V/cm}$  and  $j \leq 10 \mu\text{A/cm}^2$ ) allowed to prepare homogeneous by their composition hydrogen intercalates  $\text{H}_x\text{InSe}$  and  $\text{H}_x\text{GaSe}$  within the ranges of concentrations  $0 < x \leq 5$  for plates and  $0 < x \leq 6$  for powders of the same crystals. The hydrogen concentration was determined via the amount of electric charge passing through the sample placed into the cell. These conditions for intercalation allowed obtaining the samples of high quality, the crystal being not destroyed.

Deintercalation of hydrogen from layered intercalates of  $\text{H}_x\text{InSe}$  and  $\text{H}_x\text{GaSe}$  crystals were made for 3 to 9 hours at  $T = 110 \text{ }^\circ\text{C}$  and continuous pumping down. It enabled us to ascertain that the degree of intercalation for the samples  $\text{H}_x\text{InSe}$  increases practically in the linear manner with growth of the hydrogen concentration from 60% for  $x \rightarrow 0$  up to 75-80% for  $x \rightarrow 2$ . Further growth of the hydrogen concentration up to  $x \rightarrow 4$  shows that the deintercalation degree in  $\text{H}_x\text{InSe}$  and  $\text{H}_x\text{GaSe}$  increases up to 85%. As to powders of InSe and GaSe crystals, it was shown that the hydrogen concentration in them can reach values  $x = 5...6$ , and the deintercalation degree can do 90%. In this case, using the optical and electron-microscopic methods applied to the samples of  $\text{H}_x\text{InSe}$  and  $\text{H}_x\text{GaSe}$  intercalates, it was ascertained that repeated cycles of intercalation-deintercalation with hydrogen for concentrations  $0 < x < 2$  do not cause any visible worsening the physical parameters of InSe and GaSe crystals.

### 3. SEM investigations of InSe and GaSe layered crystals

SEM, EDS and HKL investigations of  $\epsilon$ -GaSe and  $\gamma$ -InSe single crystals as well as their hydrogen intercalates were performed using Zeiss EVO 50 XVP scanning electron microscope equipped with the detectors INCA ENERGY 450 and that for diffraction of back-scattered electrons HKL Channel 5 EBSD of the firm Oxford Instruments Analytical Ltd. The concentration of intercalated hydrogen in these samples was from  $x = 0$  up to  $x = 5$ , where  $x$  is the amount of hydrogen atoms per one formula unit of the crystal.

With this aim, we prepared 12 samples of GaSe crystals, 10 of which contained hydrogen with the concentrations  $x = 0; 0.25; 0.5; 1.0; 1.25; 1.5; 2.5; 3.0; 4.0; 5.0$ ; as well as non-intercalated GaSe crystal annealed in silica ampoule for 3 hours in vacuum at the temperature  $T = 350$  °C. Besides, we prepared the sample of GaSe crystal annealed in silica ampoule filled with gas-like hydrogen under pressure for 3 hours at the same temperature. By analogy, in the case of InSe crystals, the hydrogen concentrations were as follows:  $x = 0; 0.1; 0.2; 0.5; 0.75; 1.0; 1.25; 1.5; 1.75; 2.0$ . It should be noted that, contrary to the case of InSe crystals, after annealing the GaSe crystals we observed a red color deposit on internal surfaces of ampoules, which corresponds to polycrystalline Se films.

The performed SEM studies showed that, even at  $8 \cdot 10^4$ -fold magnification over the whole range of chosen  $x$  concentrations, electron images of crystalline surfaces did not reveal any structural defects related with introduction of hydrogen into these crystals.

Along with it, as seen in Figs. 3a and 3b for the example of the sample No 1 ( $x=0$ ), these layered GaSe crystals both non-intercalated and intercalated with hydrogen contain considerable amount of foreign spatial inclusions with dimension of 60 to 300 nm. Performed by us analogous investigations of InSe crystals did not reveal such foreign inclusions.

Complex EDS and XRD investigations enabled us to ascertain that these inclusions were present in the bulk of these crystals, and they were inclusions of monoclinic modification inherent to  $\beta$ -Se (group 2,2/m). They are located in the interlayer space of GaSe crystal. As a result of matrix pressure, lattice parameters of the foreign phase  $\beta$ -Se essentially deviate from their standard values. Note that after annealing the GaSe crystals in vacuum or hydrogen atmosphere under pressure their electron images (see Fig. 3c, sample No 11) did not contain any foreign inclusions.

In addition, low-angle XRD investigations showed that, with increasing the concentration of intercalated hydrogen, lattice parameter deviation in  $H_x$ GaSe matrix increases, too, and the lattice parameter differs from its standard value for GaSe (hexagonal group 9,6/mmm) as a consequence of hydrogen pressure on the matrix. Indeed, as it was shown in (Zhirko et al., 2007b) using the direct XRD investigations of  $H_x$ GaSe crystals at  $T = 300$  K and  $x = 1.0$ ,  $C_0$  parameter grows by  $0.031 \pm 0.003$  Å from  $C_0 = 15.94$  Å up to  $C_0 = 15.971$  Å, while the parameter  $a_0$  does by  $0.006 \pm 0.003$  Å from  $a_0 = 3.753$  Å up to  $a_0 = 3.759$  Å.

In first approximation (Zhirko et al., 2007a) assume that at low concentrations atomic hydrogen enter into the van der Waals gap by the presented on the Fig. 2c schema and creates  $H_2$  molecules that occupy an ordered positions schematically shown in Fig. 2c.

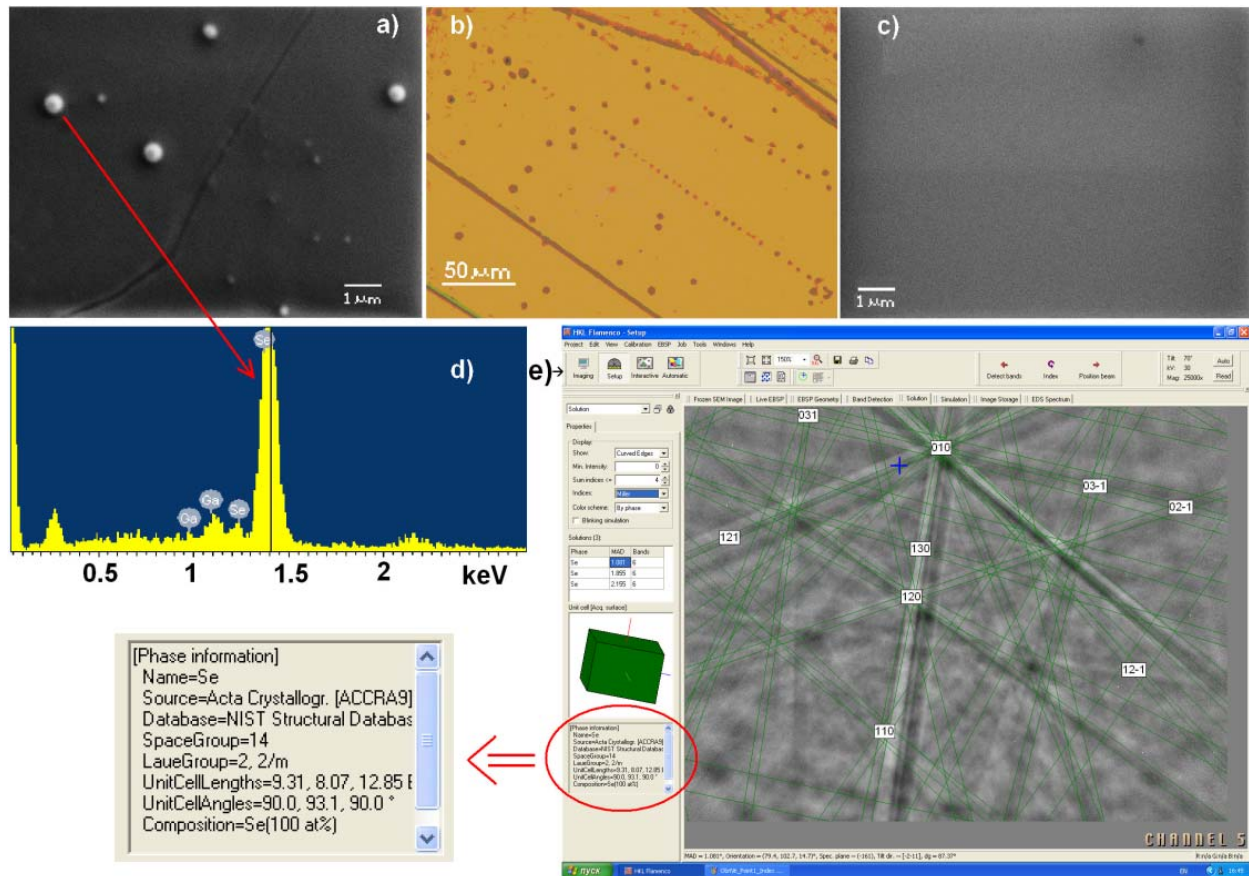


**Figure 3.** SEM images of GaSe crystals non-intercalated (a) and annealed (c) in silica ampoule for 3 hours in vacuum at the temperature  $T = 350$  °C, which are obtained at 10000-fold magnification by using Zeiss EVO 50 XVP scanning electron microscope; (b) image of GaSe crystal obtained using transmission optical microscope Carl Zeiss Primo Star 5 at 1000-fold magnification; (d) EDS spectra and (e) low-angle XRD image of foreign inclusion  $\beta$ -Se shown in Fig. 3a.

Appearance of hydrogen molecules in the gap result in occurrence of interlayer pressure and in increasing of interlayer parameter  $C_0$ . At higher concentrations atomic hydrogen incorporate into the crystal layers.

Starting from this concept, (Zhirko et al., 2007a) estimate the concentration and pressure of  $H_2$  molecules in the van der Waals gap of  $H_xInSe$  at  $x=2$ . As the volume of  $\gamma$ -InSe conventional hexagonal cell is equal  $V = 351 \text{ \AA}^3$ , the concentration of elementary cells is  $N_0 = 1/V = 2.85 \cdot 10^{21} \text{ cm}^{-3}$ . At  $x=2$ , one  $H_2$  molecule corresponds to one  $In_2Se_2$  molecule. Hence,  $H_2$  molecular concentration is equal  $N = 3N_0 = 8.55 \times 10^{21} \text{ cm}^{-3}$ . Using Clapeyron's equation for the ideal gas pressure  $P = Nk_B T$ , where  $k_B$  is the Boltzmann constant and  $T$  is the absolute temperature, (Zhirko et al., 2007a) deduce that the pressure caused by  $H_2$  molecules in InSe van der Waals gap is equal to 9.4 MPa at  $T = 80K$  and 35.4 MPa at  $T = 300K$ .

It should be mentioned that the influence of hydrostatic pressure on lattice parameters, for instance  $\gamma$ -InSe crystals, is studied rather well. In accord with (Olguin et al., 2003), growth of the hydrostatic pressure from  $10^5$  up to  $8 \times 10^9$  Pa causes essential narrowing the van der Waals gap as a consequence of decreasing the distance  $C_{Se-Se}$  from 3.8 Å down to 3.3 Å (13%)

(see Fig. 2c). In this case, the distance  $C_{\text{In-In}}$  decreases from 2.79 Å down to 2.69 Å (3.58%),  $C_{\text{In-Se}}$  from 2.65 Å down to 2.59 Å (2.26%). However, due to the angle  $\angle\varphi$  increase from 119.3° up to 121.3° (1.5%), the thickness of the crystalline layer  $C_l$  is decreased by only 0.26%, i.e. from 5.36 Å down to 5.345 Å.

Thereof, extrapolating the data of (Olguin et al., 2003) to the case when  $\text{H}_2$  molecules do not narrow but expand the interlayer space, in accord with (Zhirko et al., 2007a) one can estimate that for the pressure  $P = 35.4$  MPa ( $x = 2$ ,  $T = 300$  K – the case when each molecule in the interlayer space corresponds to one molecule  $\text{In}_2\text{Se}_2$ ) the distance  $C_{\text{Se-Se}}$  should increase from 3.8 Å up to 3.808 Å, while the constant  $C_0$  for the crystal  $\gamma\text{-InSe}$  - by  $0.024 \pm 0.01$  Å, respectively.

It should be noted that, in the case when the intercalation degree is considerable, the pressure of foreign atoms or molecules in the interlayer space can cause even exfoliating the crystals, as it takes place in graphite (Anderson & Chung, 1984). The analogous phenomenon was also observed by us in fast regimes of hydrogen intercalation in layered crystals, and hard regimes of intercalation caused destruction of crystals up to powder-like states. But we used here the specially chosen regimes that allow preparation of homogeneous samples, and multiply repeated processes of intercalation-deintercalation do not worsen parameters of InSe and GaSe crystals.

#### 4. Optical investigations of InSe and GaSe hydrogen intercalates

Optical methods of investigation as well as electron microscopy are related to non-destructive methods and bring considerable information about elementary excitations in crystals. Low-temperature measurements ( $T = 4.5 \dots 250$  K) of exciton absorption spectra of  $\text{H}_x\text{InSe}$  and  $\text{H}_x\text{GaSe}$  intercalates were made using a 0.6-m monochromator MDR-23 (LOMO, Russia) with a grating of 1200 grooves/mm. The spectral width of the slit did not exceed 0.2 meV during the experiments. Investigations of absorption spectra were made using a helium cryostat (A-255) designed at the Institute of Physics, National Academy of Sciences of Ukraine. It was equipped with a UTRECS K-43 system allowing control over sample temperature within the range of 4.2 to 350 K with high accuracy (0.1 K). A tungsten-halogen lamp was used for the absorption measurements. The photomultiplier tubes FEU-79 and FEU-62 served as a radiation detectors.

Calculations of excitonic absorption spectra inherent to  $\text{H}_x\text{InSe}$  and  $\text{H}_x\text{GaSe}$  intercalates, in accord with (Zhirko, 1999; Zhirko, 2000), were made in approximation of weak interaction of Wannier excitons with effective vibrations of crystalline lattice (with the frequency  $\Omega$ ), energy of which  $\hbar\Omega$  practically coincided with the energy of homopolar optical  $A'$ -phonon. The absorption bands for the main and excited exciton states as well as for band-to-band transitions were obtained with account of scattering by optical phonons and defects of crystalline lattice in accord with the standard convolution procedure for the theoretical value of absorption coefficient  $\alpha(\hbar\omega)$  in the Elliott model (Elliott, 1957) with the Lorentz function  $f(\hbar\omega) = \Gamma / \left[ \pi (E^2 + \Gamma^2) \right]$  in the Toyozawa model (Toyozawa, 1958), where  $\Gamma$  is the halfwidth of the exciton absorption band, which is associated with the lifetime  $\hbar/2\Gamma$ .

## 4.1. InSe hydrogen intercalates

Our studies of exciton absorption have shown that the influence of hydrogen intercalation on optical properties of  $H_x\text{InSe}$  crystals is more pronounced than that in the  $H_x\text{GaSe}$  ones. Therefore, let us first consider exciton absorption spectra of  $H_x\text{InSe}$  crystals, and then generalize the obtained conclusions to the crystals  $H_x\text{GaSe}$ .

The depicted in Fig. 4a absorption spectrum of the crystal  $H_{0.07}\text{InSe}$  is obtained at  $T = 80$  K with account of light reflection from the crystal frontal face ( $n_0 = [n_0^{\perp 2} \cdot n_0^{\parallel}]^{1/3} = 3.5$  (Zhirko, 1999)). In the same figure, we have shown the fitted absorption bands for  $n = 1$  (curve 1) and  $n = 2$  (curve 2) exciton states, band-to-band transition (curve 3) and shallow donor level (with participation of two optical full-symmetric  $A_1^{\perp 1}$ -phonons) located at  $20 \pm 2$  meV below the conduction band bottom (curve 4). The resulting fitting curve 5 was obtained with account of contribution from  $n = 1$  to  $n = 4$  exciton transitions, band-to-band transition, shallow donor and acceptor levels located by 20 meV below the conduction band bottom and by 90 meV above the top of valence band.

When using hydrogen intercalation with the concentration  $x = 0.07$  in  $H_{0.07}\text{InSe}$  crystals (see Fig. 4c), one can observe the shortwave shift of  $n=1$  exciton absorption band by 0.8 meV relatively to its position in the non-intercalated InSe crystal. Further growth of the hydrogen concentration causes a non-monotonous shift of this band as well as its maximum. For example, within the range  $0 < x \leq 0.5$  energy position of this peak is shifted by 4.5 meV from  $E_1 = 1.3275$  eV up to  $E_1 = 1.3320$  eV; while within the range  $0.5 < x \leq 1$  one can observe the decrease in energy down to  $E_1 = 1.3295$  eV; further growth of the hydrogen concentration does not lead to any change in the energy position  $E_1(x)$ .

As can be seen in Fig. 4b (curve 6), simultaneously with the shift of  $E_1$  caused by growth of the hydrogen concentration, one can also observe an increase in the halfwidth  $\Gamma_1$  for  $n = 1$  excitonic absorption band. Within the range of values  $0 < x \leq 1$ , the halfwidth  $\Gamma_1$  grows with  $x$ , and for  $x > 1$  becomes practically constant. Thus,  $\Gamma_1(x)$  dependence can be approximated by the following analytic function

$$\Gamma_1(x) [\text{meV}] = \Gamma_1 \cdot \{1 + 1/\exp[1/(\Gamma_1 \cdot x)]\}. \quad (1)$$

### 4.1.1. Discussion of the model for exciton localization in hydrogen intercalates of InSe layered crystals

Being based on the data of other authors concerning the influence of hydrostatic pressure  $P$  on the bandgap width  $E_g$  for InSe, it was shown in the work (Zhirko et al., 2007a) that the shortwave shift  $E_1$  by the value 4.5 meV for  $x = 0.5$  cannot be satisfactorily explained by dependences of the exciton binding energy  $R_0(P)$ , dielectric permittivity  $\epsilon_0(P)$  and bandgap width  $E_g(P)$  on the pressure  $P$  arising with introduction of hydrogen into the interlayer space, as their contributions  $R_0(P)$  and  $E_g(P)$  to this shift are opposite, and for  $x = 0.5$  ( $P = 2.4$  MPa) their total contribution reaches only 0.01 meV. Moreover, the dependence of exciton parameters  $E_1$  and  $\Gamma_1$  on  $x$  gives some bases to believe that this shortwave shift of exciton absorption band is caused by the  $\epsilon_0$  growth as a cosequence of hydrogen introduction into the interlayer space. In accord with the following equation

$$R_0(x)[meV] = 13605 \cdot \mu / \varepsilon_0^2(x) \quad (2)$$

it becomes apparent in lowering the exciton binding energy  $R_0$ .

For more convenient discussion, let us describe the  $\varepsilon$  growth as a result of appearance of molecular hydrogen in the interlayer space by introduction of an additional parameter  $\varepsilon^*(x)$  that grows with  $x$  and characterizes growth of anisotropy in crystal dielectric permittivity within the range comprised by the exciton:

$$\varepsilon(x) = [\varepsilon^{\perp 2} \cdot \varepsilon^{\parallel} \cdot \varepsilon^*(x)]^{1/3} \equiv \varepsilon_0 \cdot \varepsilon^*(x)^{1/3} \quad (3)$$

where the parameter

$$\varepsilon^*(x) = \prod_{j=1}^m \varepsilon_j(x) \equiv \varepsilon_i(x)^m \quad (4)$$

$m$  is the exponential index equal to the amount of interlayer spaces comprised by the exciton diameter  $d_{exc}$ ;  $\varepsilon(x)$  – dielectric permittivity of one interlayer space, which is dependent on  $x$ . In the case of non-intercalated InSe crystal, it is equal to vacuum dielectric constant  $\varepsilon(0) = \varepsilon_v = 1$ .

With account of performed estimations, the shortwave shift  $E_1(x)$  for values  $0 < x < 0.5$  (see Fig. 4c) is caused by lowering  $R_0$  from 14.5 down to 10.0 meV as a consequence of the dielectric permittivity  $\varepsilon(x)$  growth from 10.5 up to 12.6 (see the insert to Fig. 4b). It is rather well described by the following relation

$$\varepsilon(x) = 10.5 \cdot (1 + 1.5 \cdot x)^{1/3}, \quad (5)$$

represented by the curve 7. In this case, when  $\varepsilon(x)$  behavior corresponds to Eq. (5), the curve 8 in Fig. 4c describes  $R_0(x)$  dependence within the range of values  $0 < x < 2$ . It is seen that the curve 8 well describes experimentally observed  $R_0(x)$  decrease within the range  $0 < x < 0.5$ , but further we observe growth of  $R_0$ , which is caused by increasing anisotropy of dielectric permittivity  $\varepsilon$ . Indeed, in accord with Eq. (3),  $\varepsilon^{\parallel}(x)$  increases from 9.9 up to 16.9 as a consequence of the  $\varepsilon^*(x)$  parameter growth from  $\varepsilon_v = 1$  up to 1.7.

In accord with the expression

$$a_{exc} [nm] = 0.053 \cdot \varepsilon(x) / \mu, \quad (6)$$

where  $a_{exc}$  is the exciton radius, the exciton diameter grows linearly with  $\varepsilon(x)$  from 9.51 nm up to 11.43 nm, which is equivalent to increasing the exciton diameter  $d_{exc} = 11.3$  up to 13.5 crystalline layers (while the layer thickness in InSe crystal is  $d_{layer} = 8.44 \text{ \AA}$ ). Thereof, for  $m = 13$ , accordingly to Eq. (9) for  $x = 0.5$  ( $P = 2.3 \text{ MPa}$ ) and  $T = 80 \text{ K}$ , one can obtain  $\varepsilon = 1.04$ .

Analogous calculations for  $x = 1$  give the following results:  $\varepsilon = 14.25$  and the parameter  $\varepsilon^* = 2.5$ . In this case,  $R_0$  should decrease further down to the value 6.45 meB, and the exciton diameter should increase up to  $d_{exc} = 12.9 \text{ nm}$  ( $d_{exc} = 15.3$  crystalline layers). For  $m = 15$  ( $x = 1$ ,  $P = 4.7 \text{ MPa}$  and  $T = 80 \text{ K}$ ), one obtains  $\varepsilon = 1.062$ .

For  $x = 2$ , one can obtain  $\varepsilon = 16.67$  and  $\varepsilon^* = 4.0$ ,  $R_0 = 5.73 \text{ meV}$ ,  $d_{exc} = 15.1 \text{ nm}$  ( $d_{exc} = 17.9$  crystalline layers). For the value  $m = 18$  ( $x = 2$ ,  $P = 9.4 \text{ MPa}$  and  $T = 80 \text{ K}$ ), one can obtain  $\varepsilon = 1.081$ .

The performed calculations show that the value  $a$  also grows with  $x$  and begin to reach experimental values inherent to dielectric permittivity of liquid nitrogen (Malkov, 1985), which is equal to 1.253 and 1.230 for the temperatures 14 and 20.5 K, respectively.

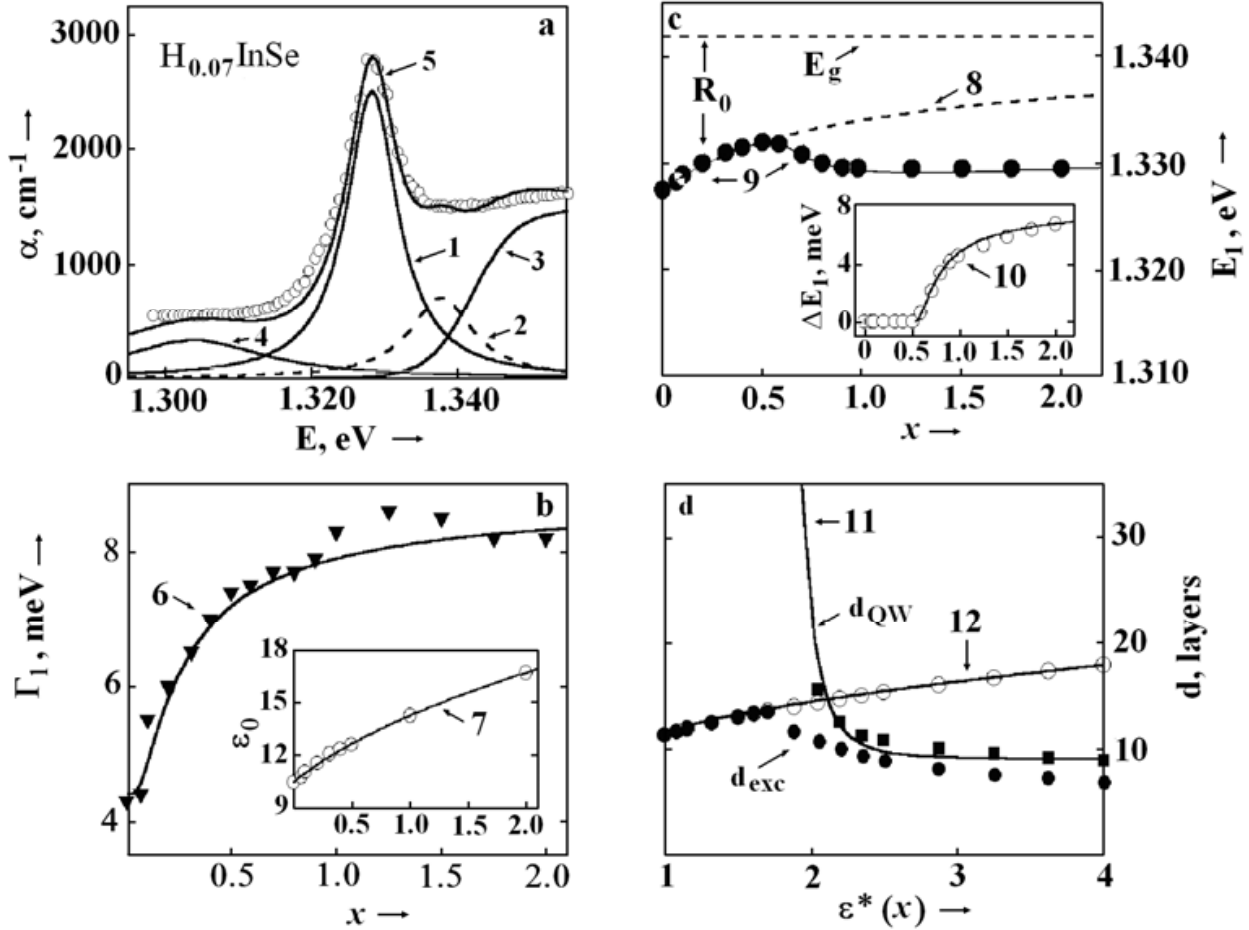


**Figure 4.** a – open circles and curve 5 – experimental and calculated spectra of exciton absorption for the crystal  $H_{0.07}InSe$  at  $T = 80$  K; b – triangles – experimental dependences for the halfwidth  $\Gamma_1$  on  $x$ . In the insert – open circles and experimental dependences of  $\epsilon_0$  on  $x$ ; c – circles – experimentally observed shift of  $n = 1$  maximum of the exciton absorption band as a dependence  $E_1$  on  $x$ . The straight line  $E_g$  shows a stable position of the bandgap energy  $E_g$  with varied  $x$ .  $R_0$  – illustrates lowering the exciton binding energy with varied  $x$  in the case when localization of excitons is not taken into account. In the insert – circles designate experimental dependences  $\Delta E_1$  on  $x$ ; d – squares – calculated values for the dependence of the quantum well thickness  $d_{QW}$  on the parameter  $\epsilon^*(x)$ . Open and filled circles – experimental dependences of the exciton diameter  $d_{exc}$  on the parameter  $\epsilon^*(x)$  with and without account of exciton localization, respectively. The curves 1 to 4 – absorption bands for  $n = 1, 2$  exciton states, band-to-band transition and shallow defect level, the curve 6 is plotted in accord with Eq. (1), curve 7 – Eq. (5), curve 8 – Eq. (2), curve 9 – with account of exciton localization inside the plane of layers, curve 10 – Eq. (8), curves 11 and 12 are built in accord with Eqs. (10) and (6).

It is noteworthy that the numeric values of parameters  $\epsilon^*$  and  $\epsilon$  versus  $x$  are well described by the following analytical dependences:

$$\epsilon^*(x) = \epsilon_v + 1.5 \cdot x \quad \text{and} \quad \epsilon(x) = \epsilon_v + 0.06 \cdot x^{1/2}, \quad (7)$$

where  $\varepsilon_v=1$ . Thereof, it is seen that growth of the dielectric permittivity in the interlayer space and within the range  $0 < x < 0.5$  corresponds to experimentally observed decrease in  $R_0$ , however, within the range  $0.5 < x < 1$  the shift of  $E_1(x)$  dependence changes its sign to the opposite one, and for  $1 < x < 2$   $E_1$  position becomes stabilized.

This  $E_1(x)$  behavior allows to assume that the parameter  $\varepsilon^*(x)$  characterizing the degree of anisotropy of dielectric permittivity in the part of medium comprised by one exciton increases in such a manner that for  $\varepsilon^* = 1.7$  ( $x = 0.5$ ) motion of excitons becomes localized within the plane of a crystalline layer. Therefore, further growth of  $\varepsilon(x)$  and  $\varepsilon^*(x)$  results in lowering the exciton radius and width of the quantum well where its localization takes place. This conclusion is confirmed by the experimental data for the dependence  $\Delta E_1(x)$  shown with open circles in the insert to Fig. 4c and described with the expression

$$\Delta E_1(x) [\text{meV}] = 13/\exp[x/2 \cdot (x-0.5)] \quad (8)$$

represented by the curve 10.

In Fig. 4d, squares show the dependence for the width of quantum well where the exciton is localized on the parameter  $\varepsilon^*(x)$ , this dependence being obtained in accord with the classic expression

$$E = \frac{\pi^2 \hbar^2}{2d_{QW}^2 M_{exc}} \quad (9)$$

and experimental data  $\Delta E_1(x)$ . For convenience, as a dimensional unit of the quantum well width  $d_{QW}$  we took the thickness of one crystalline layer, and  $M_{exc} = m_e + m_h$  is the translational mass of excitons. Open circles show the dependence of the exciton diameter  $d_{exc}$  on the parameter  $\varepsilon^*(x)$  without account of its localization inside the layer plane, while the squares do it with account of localization.

As seen in Fig. 4d, within the range of parameter values  $1 < \varepsilon^*(x) < 1.7$ , the quantum well does not arise ( $d_{QW} = \infty$ ), here one can observe the case of ordinary growth of the exciton diameter  $d_{exc}$  (open circles), which is caused by growth of  $\varepsilon(x)$ . Within the range of values  $1.7 < \varepsilon^*(x) < 2.5$ , strong localization of excitons inside the plane of crystalline layers, and the quantum well is narrowed from 107 down to 12.8 crystalline layers. Simultaneously, the exciton diameter  $d_{exc}$  decreases from 13.5 down to 8.8 crystalline layers.

In accord with Eq. (7), further  $x$  growth results in increasing the parameter  $\varepsilon^*(x)$  from 2.5 up to 4.0, which reduces the quantum well width from  $d_{QW} = 12.8$  down to 10.55 layers as well as the exciton diameter – from  $d_{exc} = 8.8$  down to 6.8 layers. The values  $R_0$  and  $d_{exc}$  are finally stabilized, and exciton motion is fully localized inside the layer plane. The experimental data for the dependence  $d_{QW}(\varepsilon^*)$ , where (see Eq. (7))  $\varepsilon^* = f(x)$ , are well described with the following analytical expression

$$d_{QW}(\varepsilon^*) [\text{layers}] = 9 + 0.4/(\varepsilon^*(x) - 1.7)^3 \quad (10)$$

that is plotted with the curve 11 in Fig. 4d.

Let us note that numeric values for  $d_{\text{exc}}$  in the case  $\varepsilon^*(x) > 1.7$  were obtained in approximation that growth of the anisotropy parameter should be accompanied with the condition  $\varepsilon(x)^m \leq 1.7$ . As far as the value  $\varepsilon(x)$  growing with  $x$  becomes higher than 1.7, the amount of layers  $m$  comprised by the exciton should decrease.

This statement is confirmed by the experimental dependence for the halfwidth  $\Gamma_1$  of  $n=1$  exciton absorption band on  $x$ . This dependence is shown in Fig. 4b. Indeed, growth of  $d_{\text{exc}}$  in the range  $x < 0.5$  results in increasing probability of exciton scattering by point defects and growth of initial values for homogeneous widening the main ( $n=1$ ) and excited excitonic states ( $n > 1$ ) at  $T = 0$  K  $\Gamma'_n(0) = g^2[\hbar\Omega(R_0/n^2 - \hbar\Omega)]^{1/2}$ . In what follows, in the range  $x > 0.5$  when the exciton dimension is stabilized inside the quantum well, the experimental dependence of the halfwidth  $\Gamma_1(x)$  goes to saturation. The curve 6 in Fig. 4b, in accord with Eq. (1), shows the dependence  $\Gamma_1(x)$  for  $\Gamma_1(T = 80 \text{ K}) = 4.4 \text{ meV}$ .

## 4.2. GaSe hydrogen intercalates

The investigation of the influence of hydrogen intercalation on optical properties of layered crystals was extended to GaSe crystals at  $T = 4.5 \text{ K}$ , as at this temperature exciton scattering is only caused by lattice defects. In this case, hydrogen molecules can be considered as some defects relatively to the proper system of elementary excitations in the crystal. Their concentration grows with  $x$ , where  $x$  is the amount of hydrogen atoms per one formula unit of the crystal.

The spectra of excitonic absorption for GaSe crystals intercalated with hydrogen in concentrations  $x = 0 \dots 0.5$  are depicted in Fig. 5 in geometry  $\vec{E} \perp C$ -axis of the crystal, at the temperature  $T = 4.5 \text{ K}$  (with account of reflection from the frontal face of the crystal). To take into account the light reflectivity, the reflection index  $n_0 = [n_0^{\perp} n_0^{\parallel}]^{1/3} = 3.1$  was determined directly from the values  $\varepsilon_0^{\perp, \parallel}$  (Zhirko, 2000), where superscripts  $\perp$  and  $\parallel$  corresponds to directions relatively to crystal optical  $C$ -axis oriented along the normal to the plane of crystalline layers.

As can be seen in Fig. 5a, near the absorption edge of non-intercalated single crystal GaSe ( $x = 0$ ) at  $T = 4.5 \text{ K}$ , one can observe the absorption bands of the main  $n=1$  and first excited  $n=2$  excitonic states, which energy positions of peaks are  $E_1 = 2.1096 \text{ eV}$  and  $E_2 = 2.1247 \text{ eV}$ , and the obtained via the wellknown relation  $E_n = R_0/n^2$  (Elliott, 1957) the exciton binding energy  $R_0 = 20.1 \pm 0.15 \text{ meV}$  corresponds to the classic value  $R_0 = 20.0 \text{ meV}$  (Zhirko, 2000) for a non-intercalated crystal GaSe.

Increasing the hydrogen concentration up to the values  $x = 1.5$  does not result in visible changes in absorption spectra. When the hydrogen concentration is further increased, essential transformation of the contour describing the  $n=1$  exciton absorption band takes place. Besides, as seen in Figs. 5e and 5f, for  $x > 1.5$  one can observe widening and energy shift of the band peak for  $n=1$  exciton state; when  $x = 2.5$  (Fig. 5c) the main excitonic state is widened, and an additional band with the peak at the energy  $E_{1'} = 2.1123 \text{ eV}$  arises near the shortwave edge of  $n=1$  absorption band. The splitting value between  $E_1$  and  $E_{1'}$  states is

equal to 2.7 meV. This formation of the additional band for the main excitonic state, when  $x$  grows, is related with creation of quasi-two-dimensional localized excitonic states splitted from the main excitonic state.

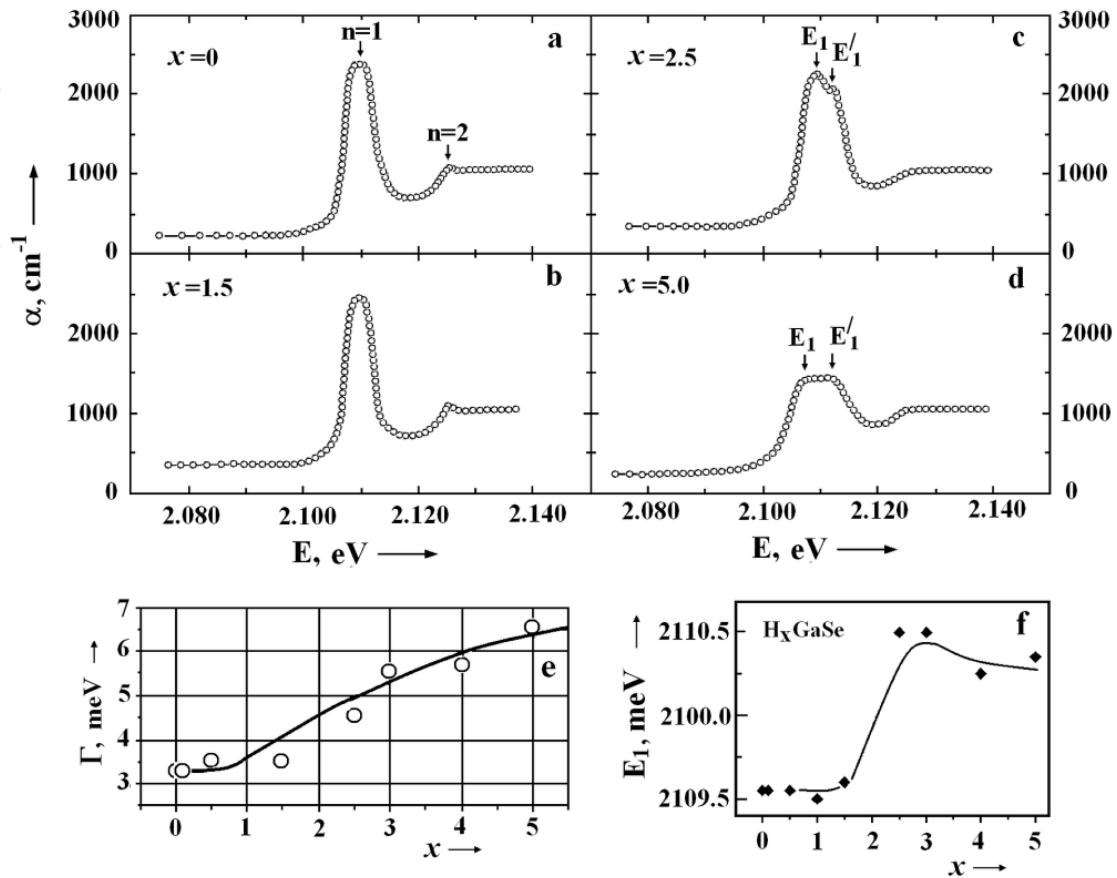


**Figure 5.** a-d –excitonic absorption spectra of GaSe crystals intercalated with hydrogen in various concentrations; e, f – dependence of the halfwidth and shift of the peak for  $n=1$  exciton absorption band in GaSe crystal on the hydrogen concentration

When  $x=5.0$ , the splitting of the main excitonic state is  $E'_1 - E_1 = (2.1117 - 2.1078) = 3.9$  meV. Our attention was attracted by the fact that the positions of peaks for the doublet main excitonic state are practically at the same distance from the peak of main excitonic state of non-intercalated crystal ( $x=0$ ). Using the known relation for the energy positions of the main and excited states in the case of quasi-two-dimensional exciton  $E_n = R_0/(2n-1)^2$  as well as experimental data for values  $E_1 = 2.1117$  eV and  $E_2 = 2.1256$  eV and  $x = 5.0$ , one can estimate the binding energy of quasi-two-dimensional exciton states in the crystal  $\text{H}_{5.0}\text{GaSe}$  as  $R_0 = 15.6$  meV.

Moreover, as seen from Fig. 5f, the energy position of the mass center of absorption band for  $n=1$  excitonic state possesses a non-linear dependence on the concentration of embedded hydrogen: when the concentration increases up to  $x=2.5$ , one can observe the shortwave shift, but in the range of higher concentrations the mass center begin to shift to low-energy side, and at  $x>4.0$  reaches saturation. Simultaneously, as seen in Fig. 5e widening the excitonic absorption band takes place.

It should be noted that the same dependences  $E_{n=1}(x)$  and  $\Gamma_1(x)$  are observed in InSe crystals intercalated with hydrogen. However, in the case of GaSe crystals they are less pronounced and observed for higher hydrogen concentrations. For instance, in HxGaSe crystals widening the main excitonic state with  $x$  growth can be approximated by the following dependence

$$\Gamma_1(x) [\text{meV}] = \Gamma_1 \cdot \{1 + 1.7 / \exp[1 / (0.1 \cdot \Gamma_1 \cdot x)]\}. \quad (11)$$

for  $\Gamma_1 (T = 4.5 \text{ K}) = 3.3 \text{ meV}$ .

This difference is caused by several reasons. The main one is as follows: the effective Bohr radius of excitons in non-intercalated GaSe crystals is 3.7 nm, and this exciton comprises 9.3 crystalline layers, while the exciton in non-intercalated InSe comprises 11.3 crystalline layers. It results in the fact that, for availability of these effects, it requires a higher hydrogen concentration in the interlayer space. The second and important reason lies in the following difference: in InSe  $\mu^\perp \epsilon_0^\perp / \mu^\parallel \epsilon_0^\parallel = 1$ , while in GaSe  $\mu^\perp \epsilon_0^\perp / \mu^\parallel \epsilon_0^\parallel > 1$ . It means that excitons in GaSe are not spherical but a little oblate in the plane of crystalline layers. It lowers the amount of layers comprised by excitons and results in lower probability of their scattering.

At the same time it was shown (Zhirko, 2011) that temperature dependences of  $n=1$  exciton band half-width in HxGaSe intercalates as well as in pure and doped GaSe and InSe single crystals attributed with exciton scattering on  $A_1^-$ -homopolar optical phonon and observed temperature increase of integral intensity of  $n=1$  exciton absorption band attributed to polariton damping by optical phonons in exciton-like states.

As a whole, one can state that intercalation of InSe and GaSe crystals results in essential transformations of their excitonic spectra. As it was shown using optical investigations, these transformations are caused by changes in the dielectric permittivity of the van der Waals gap, when it is filled with hydrogen. They manifest themselves in changing the exciton binding energy and, for sufficient degree of hydrogen intercalation, lead to further localization of exciton motion inside the plane of crystalline layers.

To check this hypothesis, we performed direct investigations of the hydrogen state in InSe and GaSe crystals by using the method of NMR spectroscopy. The respective results have been represented in the following chapter.

## 5. NMR investigations of GaSe and InSe monocrystal hydrogen intercalates and their powders

In (Zhirko et al., 2007b) the previous investigation of MNR spectra of  $H_{1.0}$ GaSe powder hydrogen intercalates were done. It was shown that NMR spectra of  $H_{1.0}$ GaSe powder under room temperature contain three bands (Fig. 6a, curve 1) associated with molecular hydrogen. In accord with the model offered in chapter 3 and with account of the band energy shift caused by the influence of matrix crystalline field on  $H_2$  molecules, these bands were identified with  $H_2$  (Fig. 6, insert) present in: i) crystal layers, where strong ion-covalent bonds are active (*L*-band); ii) interlayer space with weak van der Waals bonds (*I*-band); and iii) the regions between crystalline grains of the powder (*G*-band).

In this case, as shown in chapter 4, at low concentrations ( $x \leq 2.0$ ) molecular hydrogen is predominantly located in interlayer space, while with growing  $x$ , when this space is filled, it comes into intra-layer space. Indeed, as seen from NMR spectra of powders the integrated intensities of  $G$ ,  $I$ ,  $L$  bands for  $x = 1.0$  are in proportion 1 : 9 : 2.5 between each other. It has been also shown in (Zhirko et al., 2007b) that growth of the hydrogen concentration results in increasing  $a_0$  and  $C_0$  lattice parameters of the crystal.

In this part of our work we present a further refining of the mechanism and dynamics of hydrogen introduction into the layered crystals, which is based on additional temperature ( $T = 295...380K$ ) and polarized radiospectroscopy investigations of GaSe single crystals intercalated with hydrogen in concentrations  $x = 0...4.0$ . And at the end of this part some extrapolate conclusion on  $H_xInSe$  intercalates were done and some complement experimental NMR spectra of  $H_{1.0}InSe$  were presented.

### 5.1. Experimental part

Presented there radiospectroscopic investigation of  $H_xGaSe$  intercalates were performed using the NMR spectrometer Bruker Avance<sup>TM</sup>400. As seen from Fig. 6a, the spectra of  $H_{1.0}GaSe$  single crystals (curve 2) contain only clearly pronounced  $L$ - and  $I$ -bands inherent to molecular hydrogen located in layer and interlayer spaces, and in external magnetic field these bands are split by doublets  $L^\uparrow, L^\downarrow$  and  $I^\uparrow, I^\downarrow$ . The fact that the split value  $\Delta L > \Delta I$  also confirms conclusion (Zhirko et al., 2007b) that  $H_2$  molecules in  $H_xGaSe$  single crystals are located in two different crystal fields.

As it was shown in chapter 2 (Fig 2c), deintercalation of molecular hydrogen from layered crystals takes place at the temperature 110 °C and permanent pumping down. To study temperature influence on  $H_2$  behavior in layered crystals, we performed temperature investigations of NMR spectra for  $H_{1.0}GaSe$ . The respective data have been depicted in Fig. 6, where doublet  $I^\uparrow, I^\downarrow$  is associated with  $H_2$  located in van-der-Waals gap and (renamed here for next discussion)  $L_1^\uparrow, L_1^\downarrow$  doublet with  $H_2$  located in layer call.

To further refine the considered model for introduction of hydrogen into a layered crystal, we carried out the investigations of the influence of  $H_2$  concentrations on NMR spectra. Depicted in Fig. 6a are the NMR spectra of  $H_xGaSe$  for the concentrations  $x = 1.0$  and  $x = 4.0$  ( $T = 295 K$ ). Obtained experimental data maximum of  $I^\uparrow, I^\downarrow$  and  $L_1^\uparrow, L_1^\downarrow$  bands shifting with temperature ( $T$ ) and hydrogen concentrations ( $x$ ) was collected in Table 1.

### 5.2. Discussion

It is known that molecular hydrogen at  $T \geq 295K$  consist of para-hydrogen (25%) and ortho-hydrogen (75%) molecules. At  $T=0$  all molecules are in para-hydrogen state. Para-hydrogen possesses the total molecular spin  $S_{p-H_2} = S(+1/2) + S(-1/2) = \uparrow+\downarrow = 0$ , while ortho-hydrogen -  $S_{o-H_2} = S(+1/2) + S(+1/2) = \uparrow+ \uparrow = 1$ . In external magnetic field  $B$  the energy level of a free molecules are split by three states with spins projection  $S_{H_2} = (+1, -1, 0)$ .

x	T (K)	$I^\uparrow$ (ppm)	$I^\downarrow$ (ppm)	$\Delta I$ (ppm)	$L^\uparrow$ (ppm)	$L^\downarrow$ (ppm)	$\Delta L$ (ppm)
4.0	295	1.0	8.4	7.4	3.3	14.05	10.75
1.0	295	1.19	8.19	7.0	3.19	12.42	9.23
	310	1.22	8.10	6.88	3.0	12.12	9.02
	330	0.95	7.57	6.62	2.73	12.0	9.27
	360	0.48	6.96	6.48	2.0	11.05	9.05
	380	0.50	6.74	6.24	6.24	10.84	8.84

**Table 1.** Data for temperature and concentration dependences of the energy shift and splitting inherent to  $L$ - and  $I$ -bands observed for  $H_xGaSe$  in external magnetic field of the spectrometer Bruker Avance<sup>TM</sup> 400

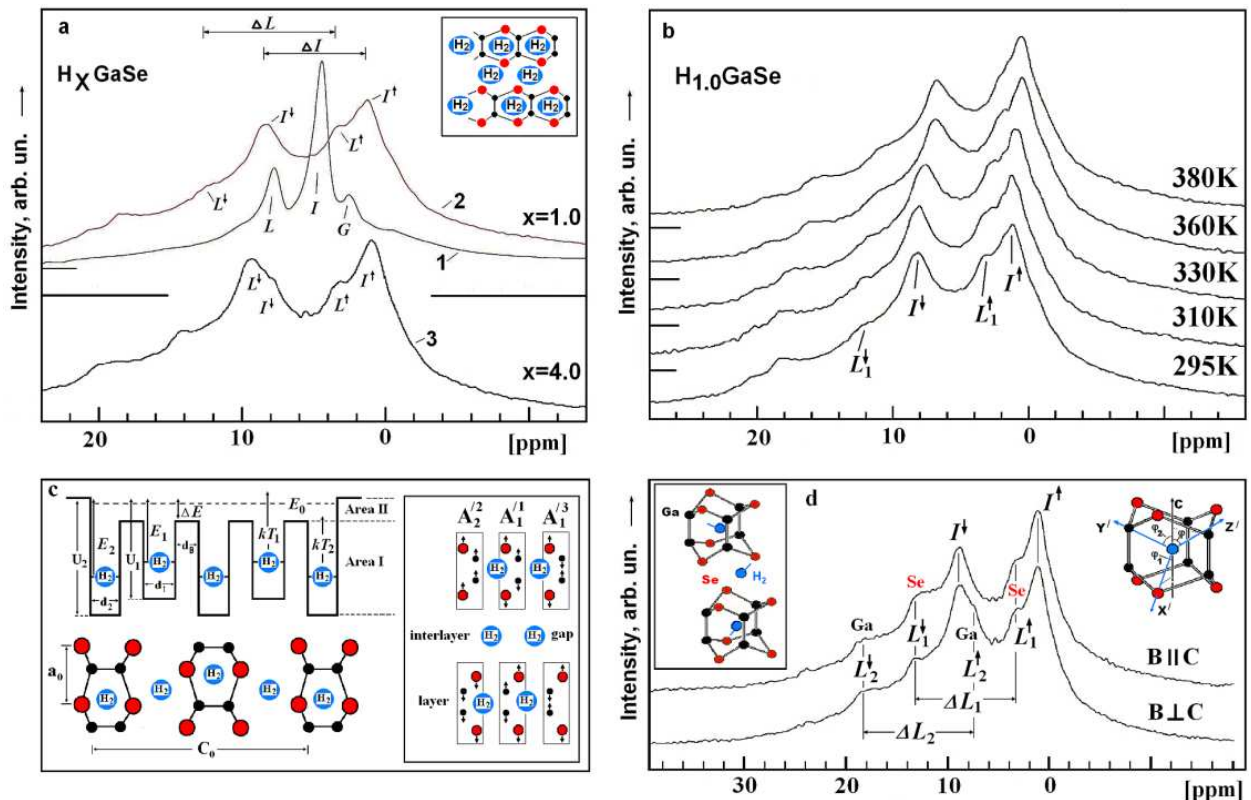


**Figure 6.** a) - NMR spectra of  $H_{1.0}GaSe$  single crystals (curve 2) and its powder (curve 1) intercalates at room temperature. Curve 3 – for  $H_{4.0}GaSe$ . Inset. 2D sketch of molecular hydrogen location in  $H_{1.0}GaSe$  powders; b) - temperature dependences of the shift and splitting of molecular hydrogen  $I$ - and  $L_1$ -bands for intercalates in  $H_{1.0}GaSe$  crystals; c) - 2D sketch and scheme of  $H_2$  1D-localization in QW's of interlayer and layer spaces of GaSe crystal at  $T=0$ . Inset. Full symmetric vibrations in  $\epsilon$ -GaSe crystal; d) - NMR spectra of  $H_{1.0}GaSe$  single crystal at  $T=295K$  for longitudinal and transverse orientation of applied external magnetic field  $B$  according to crystal axis  $C$ . Insets. 2D sketches presenting slight spin orientation of ortho-hydrogen molecules in a layer and intra-layer crystal space.

Any hydrogen molecule in crystal experiences action of a crystalline field that causes limitation of its free precession relatively to external magnetic field  $B$ , which eventually results in lowering its energy state. When measuring powder NMR spectra of  $H_xGaSe$  (analogue to the so-called «magic angle»), optical axes of crystalline grains (of  $1\text{-}\mu\text{m}$

diameter, in our case) are chaotically average oriented relatively to external magnetic field  $B$ , and in this case the total spin of all ortho-hydrogen dipole molecules in powder was equal to zero that corresponds with a para-hydrogen molecules. The bands  $G$ ,  $L$  and  $I$  observed in NMR spectra of  $H_xGaSe$  powder (Fig. 6a, curve 1) are related with resonant absorption of hydrogen molecules with total spin equal zero which are located in three different crystalline surroundings, namely: between grains, between layers and inside layers.

In the case of  $H_xGaSe$  single crystals, pronounced in the NMR spectra are two bands of molecular hydrogen located in interlayer and intra-layer spaces. In external magnetic field  $B$ , these bands are split by doublets corresponding to ortho-hydrogen which spins oriented parallel and anti-parallel to  $B$ . In our experiments, the field  $B$  is oriented in parallel to the optical axis  $C$  that is directed along the normal to layer planes in GaSe.

As seen from Fig. 6b with increasing the temperature from 295 up to 380K, one can observe the following features in NMR spectra of  $H_{1.0}GaSe$ :

- Some decrease in splitting the doublets of  $L_1$ - and  $I$ -bands,
- The very doublets of  $L_1$ - and  $I$ -bands are shifted to the side of lower energy,
- Lowering the integral intensity of  $L_1^\uparrow$ -band relatively to  $I^\uparrow$ -band.

It is also worth to note that the shift of these bands and their splitting value are in linear proportion to the inverse temperature [ $\approx const \cdot (1/T)$ ] and the constant of the temperature shift for  $L_1^\uparrow$  and  $I^\uparrow$  bands of ortho-hydrogen oriented along the field  $B$  is somewhat lower than that one for opposite orientation.

This behavior of NMR spectra is indicative of the increasing mobility of hydrogen molecules in intra-layer and interlayer spaces with increasing the temperature, which results in a reduced influence of matrix crystalline field on hydrogen. As shown by calculations within the framework of the ideal gas model (Zhirko et al., 2007a), in GaSe crystals (for  $x = 1.0$  and  $T = 300K$ ) molecular hydrogen creates the pressure in the interlayer space equal to  $P = 17.7$  MPa, which results in growth of the lattice parameter  $C_0$ . This fact is also confirmed by direct X-ray investigations (Zhirko et al., 2007b).

When  $x = 1.0$  and  $T = 380K$ , the  $H_2$  pressure value in the interlayer space is 22.4 MPa. In accord with our estimation (see chapter 2), at  $T = 384K$  (110 °C) and weak pumping down hydrogen leaves crystal: for the low concentration  $x = 0.1$ , its yield is approximately 60%, and for  $x = 4.0$ , when molecular hydrogen occupies both interlayer and intra-layer spaces, its yield reaches 85-90%.

It seems obvious to expect that growth of the hydrogen concentration resulting in the pressure increase in interlayer space and, respectively, in growing the lattice parameters  $a_0$  and  $C_0$ , should result in the increasing mobility of hydrogen in intra-layer and interlayer spaces, i.e., to drop in splitting of  $L_1$ - and  $I$ -bands as well as to their shift into the range of lower *ppm* values. However, as it can be seen in Fig. 6a, with growing the hydrogen concentration  $x$  the splitting of doublets in  $L_1$ - and  $I$ - bands is increased, and  $L_1^\uparrow$ -,  $L_1^\downarrow$ - and  $I^\downarrow$ -bands (except  $I^\uparrow$ -band) are shifted to the range of higher *ppm* values.

It is indicative of the fact that, with increasing the hydrogen concentration, the influence of matrix crystalline field on the hydrogen molecule grows, and fixed orientation of the molecule relatively external magnetic field  $B$  is kept. It should be also noted in accord with (Zhirko et al., 2007a) that for  $x \geq 2.0$  hydrogen, having filled all the translationally ordered states in interlayer space, goes into intra-layer space by virtue of quantum-dimensional effects. It also leads to a growing pressure inside crystalline layers. In this case, as seen in Fig. 6a the splitting value for  $L_1$ -band is larger than that for  $I$ -band.

### 5.3. Model for hydrogen intercalation in layered GaSe and InSe crystals

Note that even at high concentrations ( $x=4.0$ ) molecular hydrogen in the interlayer space at room temperature can be considered as condensed gas that, with the concentration growth, comes more and more into crystalline layers, which due to increased pressure enhances lattice parameters.

Performed in (Zhirko et al., 2007a) was an estimation of the level energy value for hydrogen molecule localization inside a one-dimensional well inherent to the interlayer space. In accord with the known expression

$$E_0 = \frac{\pi^2 \hbar^2}{2M_{H_2} d_z^2} \quad (12)$$

as well as values for hydrogen molecule mass  $M_{H_2} = 3673$  a.u. and width of the interlayer space  $d_z = 0.308$  nm for InSe crystal (Olguin et al., 2003), obtained was the energy of the localization level  $E_0 = 1.1$  meV. Note that the considered one-dimensional case describes appearance of the level in the interlayer space in a right manner, since motion of the molecule in the interlayer plane has a quasi-continuous spectrum.

However, the estimation of  $E_0$  value performed in (Zhirko et al., 2007a) explains localization of  $H_2$  in interlayer space only qualitatively. It is quite sufficient to consider processes of two-dimensional exciton movement in the plane of crystalline layers when hydrogen fills the interlayer space. But to explain behavior of NMR spectra for molecular hydrogen with increasing the temperature and concentration as well as its localization in inter- and intra-layer spaces, it seems no longer sufficient. Note that the localization energy for hydrogen molecules  $E_0 = 1.1$  meV obtained in (Zhirko et al., 2007a) is much less than the kinetic energies which necessary for  $H_2$  molecule to deintercalating from crystal ( $kT$  for  $T = 384$  K is equal to 33.0 meV).

With this aim, taking into account the data obtained in this work, let us refine the offered in (Zhirko et al., 2007a; Zhirko et al., 2007b) model describing intercalation and deintercalation of hydrogen in layered crystals.

For this purpose (see Fig. 6c), let us consider GaSe single crystal consisting of three cells from crystalline layers and two interlayer spaces that contain  $H_2$ . In this case, there takes place one-dimensional localization of molecules in the direction normal to layers in the

interlayer space with the width  $d_1$ . While in the planes of layers, molecular motion will be quasi-free, i.e., free for low hydrogen concentrations and strongly localized when the rest of the phase space will be practically filled with other hydrogen molecules.

For the molecule  $H_2$  present in the cell of layer space, there takes place a three-dimensional potential well with the energy of a ground localization level (111) in the case of cubic geometry (linear sizes of the well in three directions  $x, y, z$  are the same, i.e.  $d_2^x = d_2^y = d_2^z \equiv d_2$ ) that is equal

$$E_0 = \frac{3\pi^2 \hbar^2}{2M_{H_2} d_2^2} \quad (13)$$

Thus, we have a set of two type wells, namely: one- and three-dimensional ones, where the hydrogen molecule can be present, being limited with potential barriers of finite width and height. To shorten the description of  $H_2$ -molecule behavior, let us simplify the model by changing the 3D well with 1D one. As seen from Eqs. (12) and (13), at equal energies of the ground state the only well width should be changed.

With this simplification, let us construct a set of five 1D wells (Fig. 6c) separated with potential barriers. Since during intercalation the molecular hydrogen penetration into the intra-layer space is more difficult than into the interlayer one, three deeper wells correspond to localization of  $H_2$  inside crystalline layers and two more shallow - to localization of  $H_2$  in interlayer space. This area of quantum wells with localized there  $H_2$  molecules is marked in the figure as Area I. Depicted on a Fig. 6c case corresponds to the concentration  $x = 4.0$ , when  $T = 0K$ ;  $B = 0$ . The rest over-barrier phase space of the layered crystal is designated as Area II and was considered latter.

Before proceeding to calculation of well parameters in Area I, note some additional requirements:

1. When considering well geometrical parameters  $d_1$  and  $d_2$ , it is necessary to take into account the fact that the diameter of a hydrogen molecule  $D_{H_2} = 0.148$  nm is comparable with the width of interlayer space  $d_1$ . Moreover, covalent radii of selenium and gallium atoms  $R_{Se} = 0.116$  nm and  $R_{Ga} = 0.126$  nm in the layered crystal GaSe possess sizes comparable with  $D_{H_2}$ , too. The above particle sizes should be taken into account when determining the efficient geometrical sizes of wells

$$\delta_1 = d_1 - D_{H_2} \quad \text{and} \quad \delta_2 = d_2 - D_{H_2} \quad , \quad (14)$$

as well as  $d_B$  – the width of the potential barrier between them

$$d_B = [(C_0/2) - 2D_{H_2} - \delta_1 - \delta_2]/2, \quad (15)$$

where  $C_0 = 1.595$ nm (Kuhn et al., 1975) is the lattice parameter of the GaSe crystal.

2. Since the molecule spin is equal to integer (0, 1), molecular hydrogen obeys Bose statistics. Then, levels in each of the well sets are degenerated and possess the ground

level  $E_1$  for interlayer space and  $E_2$  for the intra-layer one. Assume also that in every well the hydrogen molecule possesses only localization level and  $E_2 > E_1$ . The depths of wells have finite values, and  $U_2 > U_1$ . In this case, the localization levels of  $H_2$  molecules can be found as solutions of the quadratic equation

$$E_{(1,2)} \cong U_{(1,2)} - \frac{M_{H_2} \delta_{(1,2)}^2}{2\pi^2 \hbar^2} U_{(1,2)}^2 \quad (14)$$

3. Since at  $T = 384K$  molecular hydrogen comes out of the interlayer space, let the level energy will be as  $E_1 = kT_1 = 33.0$  meV.
4. At the same time, at  $T = 384K$  and  $x = 4.0$  with a weak pumping down approximately 85% of hydrogen comes out of the crystal. Therefore, transfer of hydrogen from the intra-layer space to the interlayer one should take place at  $T \leq 384K$ , i.e.  $kT_2 \leq kT_1$ .
5. We assume that at temperatures above  $330K$  molecular  $H_2$  is in a combined state (Area II), i.e., with increasing the temperature up to  $380K$ , one can observe the only interlayer hydrogen present in a large common well. Thus, the difference between levels is  $\Delta E = E_2 - E_1 = 3.0$  meV, where  $E_2 = 36.0$  meV.

Indeed, as seen from the NMR spectra (Fig. 6b), at temperatures  $T > 330K$   $L_1^\uparrow$ -band becomes to vanish, and at  $T = 380K$  one can observe the only  $I^\uparrow$ -band that practically stops its shifting to the range of lower *ppm* values. While  $L_1^\downarrow$ - and  $I^\downarrow$ -bands caused by resonance absorption related with molecular ortho-hydrogen oriented anti-parallel to the external magnetic field  $B$  and being in more low-energy states prolong to shift with increasing temperature.

Thereof, in accord with the set  $H_2$  localization levels  $E_1$  and  $E_2$  and using the expression (14), let us determine the parameters of quantum wells in absence of external magnetic field  $B$ :

- The interlayer well depth is  $U_1 = 64$  meV, efficient width  $\delta_1 = 0.0557$  nm,  $d_1 = 0.2037$  nm,
- The intra-layer well depth is  $U_2 = 69$  meV,  $\delta_2 = 0.0533$  nm,  $d_2 = 0.2013$  nm,
- And in accord with (13a), the barrier width between them is  $d_B = 0.1473$  nm.

Note that parameters  $\delta_1$  and  $\delta_2$  obtained without any account of the experimental fact that, with increasing the temperature and hydrogen concentration in the layered crystal,  $a_0$  и  $C_0$  grow, too, which enhances the well width  $d_1$ ,  $d_2$  and changes the barrier thickness  $d_B$  in places where hydrogen is present. By other words  $d_1$ ,  $d_2$ ,  $d_B = f(T, x)$ .

### 5.3.1. The case $B=0$ , $T>0$ , $x>0$

As it was noted above, growth of the temperature forces the molecular hydrogen to come out of quantum wells to Area II and fill the phase space of the layered crystal, and for sufficient concentrations when  $x \rightarrow 4.0$  creates in it some level more  $E_0$  with the energy  $\leq 1.0$  meV. For  $x \rightarrow 0$ , the level energy  $E_0 \rightarrow 0$ :  $H_2$  behavior is close to the quasi-free one limited by the crystal bulk and atoms of its composition. By this cause, at low concentrations the hydrogen amount leaving the crystal does not exceed 60...70%, while at high concentrations it reaches 80...90%.

With increasing the temperature, the molecule kinetic energy in the well can be enhanced due to scattering at potential well walls with absorption of vibration energy quantum from crystalline lattice. When  $T = 0$ , the potential barrier walls in the first approximation are rigid and fixed (we do not take into account zero vibrations of atoms). But increase in temperature means that phonons of the crystalline lattice become active, the density of population  $n_i$  for phonon branches  $\Omega_i$  grows with temperature in accord with the law

$$n_i = \frac{1}{e^{\hbar\Omega_i/kT} - 1}. \quad (15)$$

Periodical shifts of atoms in lattice that are caused by presence of phonons, results in changing the potential barrier width  $d_B$ , which cannot but influence the energy of hydrogen molecule localization: for inelastic  $H_2$  reflection from the barrier wall (with absorption of a phonon) the molecule can pass to Area II.

The process of  $H_2$  molecule scattering by lattice vibrations will be the most efficient when: i) the molecule kinetic energy in the well is close to the phonon energy, and ii) the momentum of the molecule reflected from the barrier wall coincides (is summed up) with the barrier wall momentum (phonon momentum), which is possible when lattice atoms in the course of vibrations change the width of the potential well and barrier.

In the case of GaSe crystal, the unit cell of which consists of 8 atoms located in two crystal layers, there exist 24 normal vibrations of the lattice (Belenkii & Stopachinskii, 1983).

Three acoustic vibrations of them for  $k=0$ , where  $k$  is the wave vector of the crystal reciprocal lattice, possess the energy equal to zero and do not directly contribute to the molecule kinetic energy. All the doubly-degenerated  $E$ -vibrations also do not essentially contribute to the molecule kinetic energy, as they do not take part in significant changing  $d_1$ ,  $d_2$  and  $d_B$  width. Only three transverse (totally symmetrical)  $A$ -vibrations can provide direct contribution to changing the molecule kinetic energy because they can change quantum well width. Motion of atoms during this vibration is shown on Insert of Fig. 6c.

The first totally symmetrical  $A_{2/2}$ -vibration (interlayer) is not valid here, because: i) it possesses the low energy ( $40 \text{ cm}^{-1}$ ) to scatter molecule from quantum well; ii) interlayer space is changed, but the thickness of the crystalline layer (barrier width  $d_B$  and  $d_2$ ) remains constant.

The second  $A_{1/1}$ -vibration (half-layer with energy  $133 \text{ cm}^{-1}$ ) can change width  $d_1$ ,  $d_2$  of quantum wells but remain unchanged barrier width  $d_B$  between them. It was an active at  $T = 300\text{K}$  to take part in molecule scattering from both type quantum wells.

The third  $A_{1/3}$ -vibration (intra-layer with energy  $307 \text{ cm}^{-1}$ ) are realized with changing both the volume of the crystalline layer cell and the thickness of the interlayer space, but  $A_{1/3}$ -vibration is still insufficiently active even at temperatures close to  $380\text{K}$ .

Therefore, we assume that the totally symmetrical half-layer  $A_{1/1}$  -vibration takes main part in the processes of hydrogen molecule scattering in the wells of two kinds, besides even at

sufficiently low temperatures (150 to 200K) it promotes H<sub>2</sub> molecule tunneling from one well to another. Also, this vibration takes very active part in the processes of exciton decay (Zhirko, 2000).

### 5.3.2. The case $B \neq 0, T > 0, x > 0$

As seen from Figs. 6d and 7, the application of external magnetic field  $B$  results in vanishing degeneration and splitting of the ortho-hydrogen molecule level in every well: there arise doublets of  $L_1$  and  $I$ -bands for ortho-hydrogen molecules in NMR spectra of H<sub>x</sub>GaSe crystals, these molecules being in two different crystalline fields. Energy levels of para-hydrogen molecules with zero spin (not observed in NMR spectra of single crystal) remain the same.

At the same time as molecular hydrogen in a gaseous-like state possess diamagnetic properties the amount of ortho-hydrogen molecules oriented in parallel and anti-parallel direction to applied external magnetic field  $B$  must be equal one to another. Really on the Fig. 6d one can see that the summarized integral intensities of  $I^\uparrow$  and  $L^\uparrow$  bands for ortho-hydrogen oriented along  $B$  are in well coincidence with summarized integral intensities of  $I^\downarrow$  and  $L^\downarrow$  bands for ortho-hydrogen oriented opposite  $B$ .

Finally the NMR investigations of H<sub>1.0</sub>GaSe single crystals at T=295K with different orientation of external magnetic field  $B \perp C$  and  $B \parallel C$  (where  $C$  is a crystal axis oriented normally to crystal payer plane) were conducted. Experimental data (see Fig. 6d) cannot find energetic shift of H<sub>2</sub> absorption bands maximums with changing  $B$  orientation. But at the same time slight redistribution of integral intensities for  $I$  and  $L_1$  bands occurred. Thus in  $B \perp C$  geometry  $I^\downarrow$ -band increased and are compatible (in intensities) with  $I^\uparrow$ -band but  $L_1^\downarrow$ -band decreased. For  $B \parallel C$  geometry their mutual redistribution are reciprocal.

Also in geometry  $B \perp C$  we can clearly observe additional one doublet of  $L_2^\uparrow$  and  $L_2^\downarrow$  bands. Note that these additional  $L_2^\uparrow$  and  $L_2^\downarrow$  bands also observed in Figs. 6a and 6b but they are not so pronounced because of some intermediate  $B \angle C$  geometry. It is important that  $L_2$  doublet has greater shift than  $L_1$  doublet and  $\Delta L_2 > \Delta L_1$ .

Two  $L_1$  and  $L_2$  absorption doublets for hydrogen molecule in a crystal layer evidenced about presence of two different position of H<sub>2</sub> inside a crystal cell. Really in layer space (see inserts of a Fig. 6d) for H<sub>2</sub> molecule located in center of a cell there are two environments consisting from atoms Ga and Se. The nearest sub-lattice consisted from Ga atoms give the greatest contribution of a crystal field into chemical shift and is identified by us to a doublet  $L_2$ . The Se atoms are removed further from the centre of a cell: therefore contribution of Se atoms in chemical shift is less. We identify the contribution of Se atoms sub-lattice to a doublet  $L_1$ . For everyone sub-lattice there are three equivalent dislocations of a ortho-hydrogen molecule along an  $C$  axis and three in opposite.

With nearest-neighbour distances  $d$  obtained in (Olguin et al., 2003) for InSe:  $d_{\text{In-In}} = 2.79\text{\AA}$ ;  $d_{\text{In-Se}} = 2.65\text{\AA}$ ;  $\angle \varphi = 119^\circ 30'$ , layer thickness  $d_l = 5.36\text{\AA}$ , the distance between layers  $d_i = 3.08\text{\AA}$  and their interlayer distance  $d_{\text{Se-Se}} = 3.80\text{\AA}$ ., one can find an angle  $\angle$  between optical axis  $C$

and nearest Se ( $\angle\varphi_1$ ) and Ga ( $\angle\varphi_2$ ) atoms by values  $\angle\varphi_1 = \pm 40^\circ 45'$  and  $\angle\varphi_2 = \pm 59^\circ$  respectively.

To define orientation of hydrogen molecule in interlayer space it is essential that each layers are shift one to another and angle of Ga-Ga-Se bound in layer is about  $120^\circ$ . In this circumstance angles in Ga and Se directions are degenerated, equal to  $\angle\varphi = \pm 52^\circ$  and have an intermediate value between  $\angle\varphi_1$  and  $\angle\varphi_2$  angles.

As it is seen on Fig. 6d intra-layer doublets  $L_1$  and  $L_2$  also differently react to a direction of an external magnetic field  $B$  concerning axis  $C$ . So in geometry  $B \perp C$  doublet  $L_2$  are more pronounced, and for  $B \parallel C$  geometry  $L_1$  bands are more appreciable. It allows us to make a conclusion that spin orientation of  $H_2$  inside a layer in sub-lattices Ga and Se try to compensate each other in external magnetic field  $B$ . It is possible only in that case, when  $H_2$  spins in Ga and Se sub-lattices have opposite directions concerning axis  $C$ . Thus in absence of an external magnetic field  $B$  a corner of a spin inclination concerning an axis  $C$  in direction to Se atom is negative  $\angle\varphi_1 = - 40^\circ 45'$  and in direction to Ga atom is positive  $\angle\varphi_2 = +59^\circ$  respectively. In this case as it is seen on an inserts of a Fig. 6d corner between  $H_2$  spins in Ga and Se sub-lattices with good accuracy are equal to  $90^\circ$  and their summarized projection on axis  $C$  are negative.

In interlayer space at  $B=0$  an angle between spin of ortho-hydrogen molecule and axis  $C$  was positive and  $\angle\varphi = +52^\circ$ . In the whole three various directions of  $H_2$  spins orientation in GaSe made a right-hand rectangular system of coordinates, which allow compensate  $H_2$  spins in absence of external magnetic field  $B$ . Presented on Fig. 6d schema of  $H_2$  molecule spin projection clearly shown the reason of  $I$ ,  $L_1$  and  $L_2$  – band doublets redistribution with changing  $B$  orientation according to axis  $C$ .

Finally, using the data obtained as a result of these investigations, in Fig. 7 we have shown the scheme of splitting the level of a hydrogen molecule in  $H_xGaSe$  single crystals and powders in external magnetic field  $B$  with changing temperature and hydrogen concentration.

In insert the scheme of hydrogen molecule localization in layer and interlayer quantum wells with account of two Ga and Se sub-lattices of a layer cell are proposed. The given scheme consists of 1D interlayer QW, projection of a 3D crystal cell QW and potential barrier between them, which becomes transparent enough at high  $kT$ .

The scheme allows to:

- i. show splitting of  $H_2$  ground state in 3D QW at  $B=0$  and  $B>0$  due to different crystal field of a nearest Ga and Se atomic sub-lattices constituting crystal cell,
- ii. differentiate phase spaces of hydrogen molecule located in 1D and 3D QW and,
- iii. demonstrate process of hydrogen exit from 3D to 1D QW with growing  $kT$ .

In this case when  $H_2$  molecule exit from 3D to 1D QW it loses energy and localized in interlayer 1D QW. Accordingly the process of hydrogen entry in crystal cells occurs at high enough temperatures and concentration that allows to overcome a potential barrier created by atoms of a crystal cell. Nevertheless some part of hydrogen molecules at deintercalation remains localized in crystal cells.

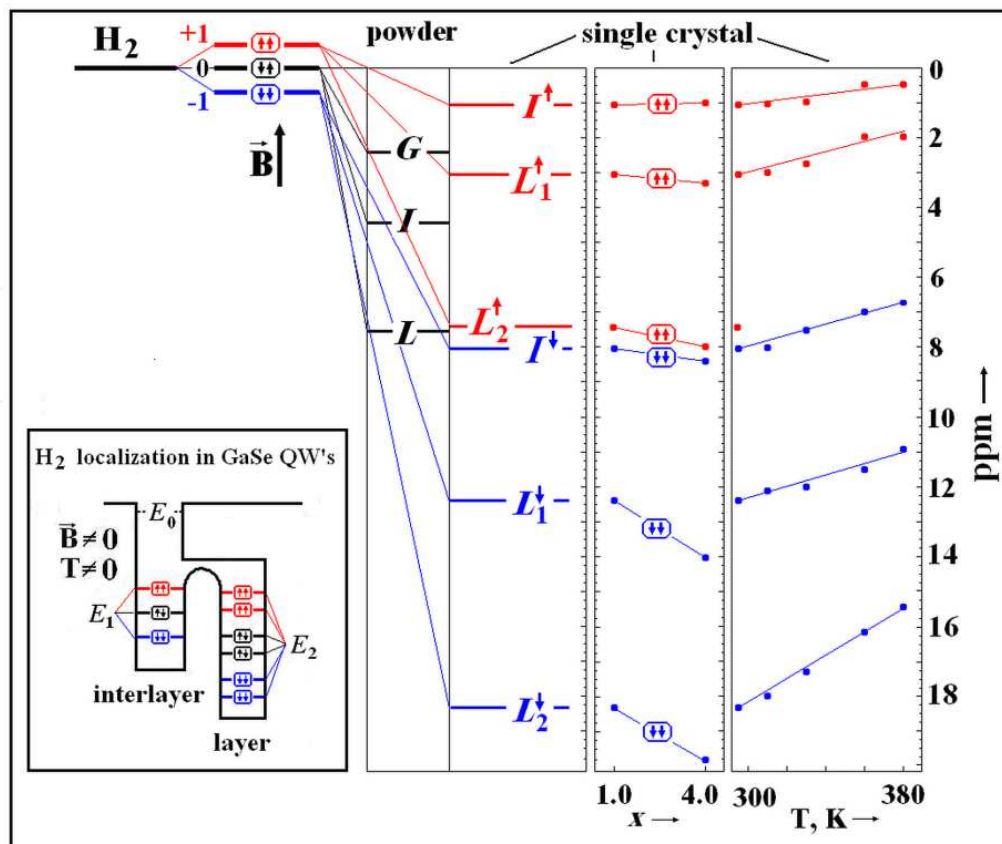


**Figure 7.** Scheme of splitting the level of a hydrogen molecule in  $H_xGaSe$  single crystals and powder in external magnetic field ( $B$ ) with changing the hydrogen concentration ( $x$ ) and temperature ( $T$ ).

Also at large hydrogen concentration and high temperatures, when hydrogen molecules are not located in QW's and possess high kinetic energy in volume of interlayer space appearance of an additional quasi-local level with energy  $E_0$  is possible.

In Introduction, we added the lattice parameters for InSe and GaSe crystals. As in InSe crystals the lattice parameter  $a_0$  and the width of the van der Waals gap are larger than those in GaSe crystals, it should be expected that the increase of the lattice parameter and interlayer space taking place in InSe as compared to GaSe crystals will result in increasing the halfwidth of  $H_2$  bands in NMR spectra and to reduction of their chemical shift and splitting.

Indeed, as seen in Fig. 8 added for  $H_{1.0}InSe$  single crystal there observed is practically 30% decrease in splitting and simultaneous growth of the width of NMR bands corresponding to hydrogen molecules. It is indicative of a decreased matrix influence on the hydrogen dissolved in it.

## 6. Electrophysical and EPR investigations of hydrogen intercalates in InSe and GaSe crystals

In what follows, we shall describe in brief some electrical properties of InSe and GaSe crystals, their hydrogen intercalates and related with it electron paramagnetic resonance (EPR) investigations of hydrogen in these crystals.

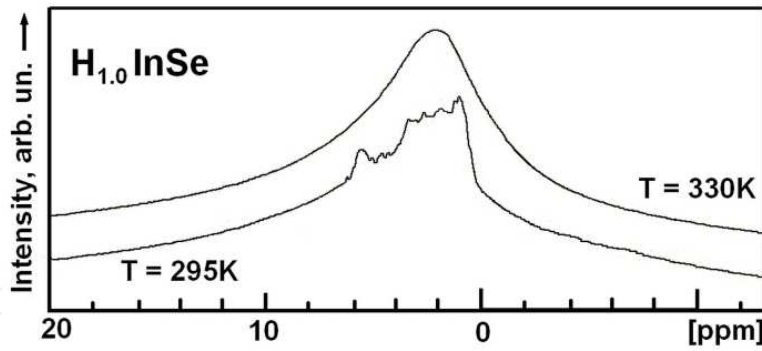


**Figure 8.** NMR spectra for  $H_{1.0}InSe$  crystal at  $T=295K$  and  $T=330K$ .

Contrary to GaSe crystals that are high-ohmic semiconductors of  $p$ -type conductivity, InSe crystals are low-ohmic and possess  $n$ -type conductivity. It enables to determine the carrier concentration in InSe crystals by using the Hall effect. As it was shown in (Zhirko et al., 2010) (see Fig. 9a), the concentration of free electrons in  $n$ -InSe at  $T = 80 K$  increases from  $n=1.5 \cdot 10^{15} \text{ cm}^{-3}$  up to  $1.4 \cdot 10^{16} \text{ cm}^{-3}$  even for comparatively low hydrogen concentrations ( $x=0.05$ ).

In addition, contrary to pure InSe crystals, the concentration of carriers does not grow with temperature in  $H_{0.05}InSe$  intercalates. Moreover, in these intercalates at  $T \approx 290 K$  one can observe the so-called “exhaustion” of the level caused by transition of electrons from the donor level into the crystal conduction band. Thereof, using the expression

$$(T_d / 300)^{3/2} = (m_0 / m_e^*)^{3/2} \cdot 4 \cdot 10^{-18} N_d, \quad (16)$$

that relates the carrier concentration with the temperature of their exhaustion  $T_d$  (290 K for  $H_{0.05}InSe$ ), and the experimentally registered electron concentration  $N_e = 1.4 \cdot 10^{16} \text{ cm}^{-3}$ , one can determine the effective electron mass value  $m_e^* = 0.152m_0$  that is in satisfactory coincidence with the value  $m_e^* = (0.143m_{0||} \cdot 0.156m_{0\perp})^{1/3} = 0.15m_0$  based on experimental data (Kuroda & Nishina, 1980).

As the electron concentration does not visibly grow in  $H_xInSe$  at  $T > 80 K$ , one can estimate the activation energy of the donor level in this crystal as 5 to 7 meV. Besides, in InSe crystals at 80 K the electron concentration is less by one order than that in intercalates and, as seen in Fig. 9a, grows with temperature. It allows drawing the conclusion that introduction of hydrogen causes a decrease in the activation energy for the shallow donor level (see Fig. 9c) that is located in InSe by 16 to 20 meV below the conduction band bottom (Martinez-Pastor et al., 1992), while the concentration of its carriers reaches  $10^{15} \text{ cm}^{-3}$ .

Further investigations of free carriers in hydrogen intercalates of  $n$ -InSe and  $p$ -GaSe crystals were performed with the method of EPR spectroscopy (Bruker X-Band Fourier Transform EPR Spectrometer ELEXSYS E 580-10/12). The experimental data have been summarized in Fig. 9b. It is seen that for  $T = 120 K$  the halfwidth of EPR-line and  $g$ -factor of the hydrogen

unpaired electron in  $H_xGaSe$  intercalates ( $g = 2.40$ ,  $\Delta H = 1500$  Gs) are higher than those in the  $H_xInSe$  ones ( $g = 1.87$ ,  $\Delta H = 60$  Gs). It is indicative of the fact that hydrogen passivation of donor type point defects in  $n$ -InSe and those of acceptor type in  $p$ -GaSe differs to some extent. For comparison, represented in Fig. 9d are the simplest defects by Schottky, which results in creation of donor and acceptor centers in  $n$ -InSe and  $p$ -GaSe crystals, respectively.

To explain this difference between EPR spectra, let us assume that during intercalation some part of hydrogen atoms located within the range of point and spatial defects of the crystal (where present are broken chemical bonds caused by absence of atoms) do not recombine to  $H_2$  molecules but are sorbed inside the range of these defects, which results in passivation of them with their proton  $H^+$  or electron  $e$ .

It is noteworthy that, contrary to graphen where hydrogen atoms break the double carbon  $C=C$  bond, which transforms it to graphan, hydrogen does not break the double  $In(Ga)=In(Ga)$  bond inside crystalline layer, as it does not form chemical compounds with In and Ga atoms.

Therefore, we assume that one of the main reasons for this difference between EPR spectra of hydrogen unpaired electrons in  $H_{1.0}InSe$  and  $H_{1.0}GaSe$  crystals is the charge state of defects. On the Fig.9d one can see the simplest defects of a donor and acceptor type in GaSe and InSe crystals. In the case of a donor the crystalline matrix within the

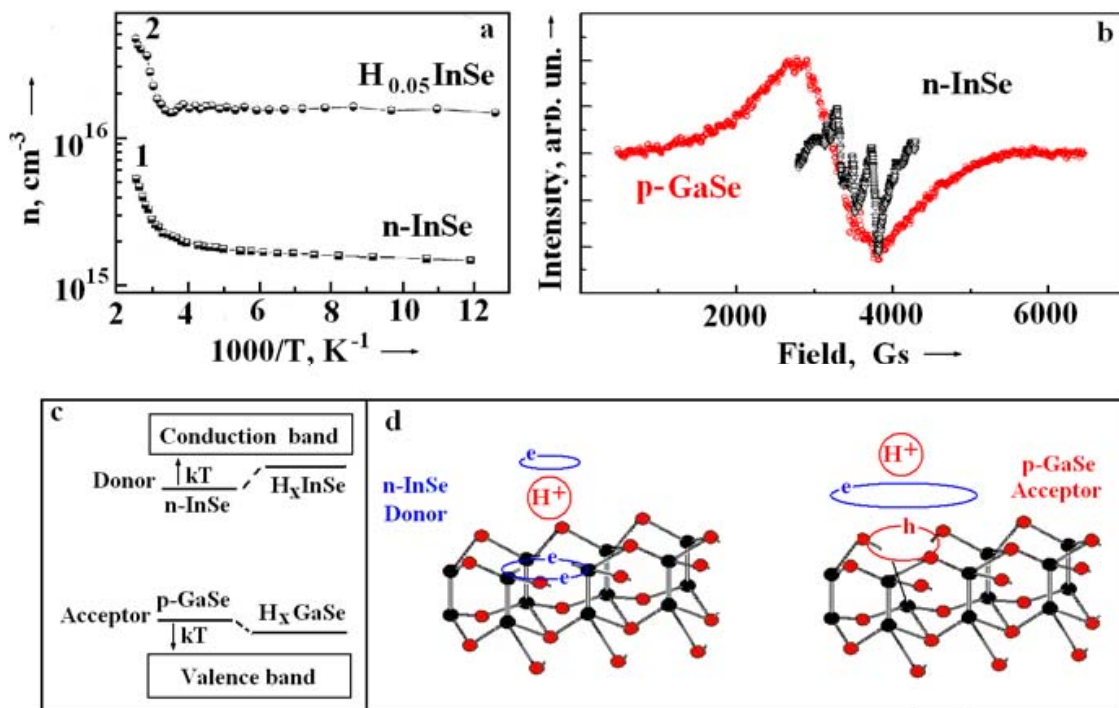


**Figure 9.** a) - Temperature dependence of free electron concentration for undoped InSe and hydrogen intercalated InSe with  $x=0.05$ ; b) - EPR spectra for  $H_{1.0}GaSe$  (red circleles) and  $H_{1.0}InSe$  (black squares) crystals obtained at 120K; c) - Change of donor and acceptor energy level displacement in forbidden gap of  $n$ -InSe and  $p$ -GaSe crystals after hydrogen intercalation; d) - A simple defect of donor and acceptor type in  $n$ -InSe and  $p$ -GaSe crystals and scheme of their hydrogen passivation.

defect range (due to absence of a Se atom) has two excess electrons that attracts by their Coulomb potential a positively charged proton from hydrogen, while the unpaired electron of the latter being captured in the proton field in accord with the scheme: donor (2e) - proton – electron. In the case of acceptor, the excess hole (absence of Ga atom) of the crystal due to its Coulomb potential attracts the hydrogen unpaired electron, on the opposite side of which the proton rotates in accord with the scheme: acceptor (h) – electron – proton.

Since the proton mass is 1836 times higher than that of electron, it is obvious that, in the case of donor, the proton (and, in general, the hydrogen atom) should be less mobile than in the acceptor case. The second reason for the difference in EPR spectra can be possibly as follows. Geometrical dimensions of the acceptor can be higher than those of donors, which is able to result in increasing the mobility of hydrogen atom inside the defect range.

The described above mechanism for hydrogen passivation of point defects (free radicals) as it is shown on a Fig. 9c should also lead to decreasing the activation energy for carriers (electrons, holes) in the crystal and increasing the concentration of carriers at low temperatures, which follows from the experimental data for  $H_{0.05}InSe$  crystals as compared to non-intercalated InSe crystals.

In addition, our calculations show that the concentration of atomic hydrogen adsorbed by defects of crystalline layers is 4...5 orders less than that of molecular hydrogen, and it is comparable with the concentration of intrinsic defects in the crystalline structure.

## 7. Conclusion

The performed complex electron-microscopic SEM, EDS, HKL, electrophysical (Hall effect), microwave (EPR, NMR) and optical-and-spectral (exciton absorption) investigations of processes for hydrogen intercalation in layered crystals InSe and GaSe enabled us to ascertain the following features.

In the course of intercalation atomic hydrogen recombine to the molecular state, occupies interlayer space of a crystal, and due to quantum-dimensional effects with increase of hydrogen concentration comes into the interstitial space, occupies centers of crystalline layer cells where its recombination to molecular state takes place.

It results in localization of hydrogen molecules, which, in its turn, leads to growth of lattice parameters  $a_0$  and  $C_0$ . At the same time, very small fraction of hydrogen ( $\approx 0.001\%$ ) in  $H_xInSe$  and  $H_xGaSe$  intercalates, being in atomic states, passivate point and spatial lattice defects, too. Simultaneously, due to decreasing the defect activation energy the concentration of free carriers increases by one order.

It is shown that, in absence of an external magnetic field  $B$ , molecular hydrogen as diamagnetic gas (owing to symmetry of the crystal and nearest nuclear environment) forms

in GaSe and InSe crystals three spin sub-lattices where spins are located mutually-perpendicularly to each other and form right-hand rectangular system of coordinates. At  $B = 0$ , the total projection of two spins inside the layer is as a whole located against the optical axis  $C$ , and between layers along the axis  $C$ .

Offered is the scheme of 1D and 3D quantum wells (QW's) that is capable to explain localization of hydrogen molecules in layered crystals in the course of intercalation as well as mechanism of their deintercalation from the crystals with participation of totally symmetrical lattice  $A_{1g}$ -phonons taking part in scattering of molecules and in formation of oscillating parameters of potential barriers and QW's. In addition, described is the mechanism of  $H_2$  scattering by  $A_{1g}$ -phonons in QW's.

Increasing the lattice parameter and width of the van der Waals gap results in decreasing the matrix influence on behavior of molecular hydrogen dissolved in it. It can be observed as a decreasing chemical shift and splitting the level of ortho-hydrogen molecule in magnetic field as well as widening the absorption bands.

Our optical investigations enabled us to ascertain that appearance of molecular hydrogen in the interlayer space of InSe crystals results in non-monotonous dependence of the exciton binding energy on the hydrogen concentration as a consequence of growth of the crystal dielectric permittivity  $\epsilon_0$ . It has been shown that, for low hydrogen concentrations, the growth of the anisotropy parameter for the dielectric permittivity  $\epsilon^*(x)$  both along layers and along the normal to them manifests itself as a decrease in the exciton binding energy  $R_0$ . In the case of further growth of the parameter  $\epsilon^*(x)$  up to the critical value  $\epsilon^* \leq 2$ , there arises 2D localization of the exciton motion inside the plane of crystalline layers, which is accompanied by growth of  $R_0$  and decrease and, in what follows, stabilization of linear dimensions both of the exciton and quantum well. As a consequence of the difference between exciton diameters in GaSe and InSe crystals ( $d_{exc}^{GaSe} < d_{exc}^{InSe}$ ), non-linear behavior of the exciton binding energy in GaSe is slower and weaker pronounced.

The performed investigations have shown that the degree of hydrogen electrochemical intercalation of layered crystals GaSe and InSe can reach the concentration  $x = 5.0$ , where  $x$  is the amount of hydrogen atoms embedded to the crystal per one its formula unit. Deintercalation of molecular hydrogen from  $H_xInSe$  and  $H_xGaSe$  crystals is realized for 3 to 9 hours at the temperature  $T = 110^\circ C$  and continuous pumping down. The degree of deintercalation grows practically linearly from 60% at  $x \rightarrow 0$  up to 80...85 % at  $x \rightarrow 4$ . Our investigations of intercalation-deintercalation processes in powders of these crystals with sizes of faces 1...20  $\mu m$  have shown that the hydrogen concentration can reach the values  $x = 6.0$ , while the degree of deintercalation can reach 90 %. The repeated cycles of soft intercalation-deintercalation regimes do not lead to essential worsening the physical parameters of InSe and GaSe crystals. At the same time hard regimes of intercalation caused destruction of crystals up to powder-like states.

## 8. Afterword

The investigations performed by us enabled to draw the conclusion that these crystals and their powders are able to take and return hydrogen in its molecular form very well, keeping at the same time their initial physical-and-chemical properties. The calculations performed in (Zhirko et al., 2007a) have shown that the pressure of molecular hydrogen inside the van der Waals gap at room temperature for  $x = 2.0$  is close to 35.4 MPa (354 atm.), which is quite comparable with the hydrogen pressure in the vessels of high pressure (400...500 atm. at -30 ... +40 °C). Moreover, an important advantage of all the hydrogen solid-state storages is their safety when storing, as compared to the above vessels.

The hydrogen content in layered intercalates of InSe and GaSe crystals is also comparable in mass fractions with that in vessels of high pressure. For example, when the pressure in these vessels reaches 500 atm., the mass fraction of hydrogen is close to 11%, while in  $H_{5.0}GaSe$  – 3.3% and in  $H_{5.0}InSe$  – 2.6%. These values are comparable with those in metal hydrides:  $BeH_2$  – 18.28%,  $LiH$  – 12.7%,  $MgH_2$  – 7.6%,  $NaH$  – 4.2%, as well as in hydrides of intermetallic compounds:  $LaNi_5H_6$  – 1.5%,  $TiFeH_2$  – 1.8%,  $Mg_2NiH_2$  – 3.8%,  $CeCo_3H_{4.5}$  – 1.4%.

An important factor promoting hydrogen intercalation in layered crystals GaSe and InSe is that molecular hydrogen at temperatures below its melting temperature (<14 K), being in the solid state, possesses dense hexagonal lattice of the spatial group  $D_{6h}^4$  ( $C6/mmc$ ) with the following parameters:  $a_{H_2}=3.75\text{Å}$  and  $C_{H_2}=6.12\text{Å}$  (Ormont, 1950). Note that the parameter  $a_{H_2}=3.75\text{Å}$  of dense hexagonal stacking for crystalline molecular hydrogen practically coincides with the parameter  $a_0=3.755\text{Å}$  (Kuhn et al., 1975) inherent to hexagonal stacking for the GaSe crystal lattice and is only a little less than that parameter  $a_0=4.001\text{Å}$  (Goni et al., 1992; Olguin et al., 2003) for InSe crystal.

It provides good conditions for location of hydrogen molecules inside centers of hexagonal cells within crystalline layers and interlayer spaces in GaSe and InSe crystals. However, the parameters  $C_{GaSe} = C_0/2 = 7.98\text{Å}$  for GaSe crystal and  $C_{InSe} = C_0/3 = 8.44\text{Å}$  for InSe crystal exceed the parameter  $C_{H_2}$  for crystalline hydrogen by 1.3 and 1.4 times, respectively. Besides, with account of the dielectric permittivities of crystals InSe ( $\epsilon_0 = 10.5$ ) and GaSe ( $\epsilon_0 = 9.8$ ), one can assume that availability of the matrix crystalline layer between two molecular monolayers of hexagonal densely stacked hydrogen in the gap as well as its presence inside centers of crystalline layer hexagonal cells should result in screening the interaction of hydrogen molecules. As a consequence, it should cause growth of the parameter  $C_{H_2}$  and its approaching to the parameters  $C_{GaSe}$  and  $C_{InSe}$  inherent to these crystals.

The performed investigations also provide the possibility to search more suitable layered structures with the aim to apply them for keeping hydrogen in various aggregate states.

## Author details

Yuriy Zhirko

*Institute of Physics of the National Academy of Sciences (NAS) of Ukraine, Ukraine*

Volodymyr Trachevsky

*Institute for Physics of Metal NAS of Ukraine, Ukraine*

Zakhar Kovalyuk

*Chernivtsy Department of Institute of Material Science Problems NAS of Ukraine, Ukraine*

## Acknowledgement

The authors express their sincere gratitude to Dr. Tkach V. N., Dr. Klad'ko V.P., Ph.D. Shapovalova I.P., Ph.D. Pyrlja M.M., Vorsovskii A.L., Zaslونkin A.V., Boledzyuk V.B. & Mel'nik A.K. who took part in performing the experiments discussed in this work.

## 9. References

- Anderson, S.H. & Chung, D.D.L. (1984). Exfoliation of intercalated graphite. *Carbon*, Vol.22, No3, pp.253-263
- Belenkii, G.L. & Stopachinskii V.B. (1983). Electronic and vibration spectra of A<sup>3</sup>B<sup>6</sup> layered semiconductors. *Uspekhi Fizicheskikh Nauk (in Russian)*, Vol.140, No2, pp. 233-270
- Elliott, R.J. (1957). Intensity of optical absorption by excitons. *Phys. Rev.*, Vol.108, pp.1384-1389
- Ghosh, P.H. (1983). Vibrational spectra of layer crystals. *Applied Spectroscopy Review*, Vol.19, No2, pp.259-323
- Goni, A.; Cantarero, A.; Schwarz, U.; Syassen, K. & Chevy, A. (1992). Low-temperature exciton absorption in InSe under pressure. *Phys. Rev. :B*, Vol.45, No8, pp.4221-4226
- Grigorchak, I. I.; Zaslونkin, A. V.; Kovalyuk, Z. D. et al. (2002). Patent of Ukraine, Bulletin No5, No46137
- Kozmik, I.D.; Kovalyuk, Z.D.; Grigorchak I.I. & Bakchmatyuk, B.P. (1987). Preparation and properties of hydrogen intercalated gallium and indium monoselenides. *Izvestija AN SSSR Inorganic materials. (in Russian)*, Vol .23, No5, pp.754-757
- Kuhn, A.; Chevy, A. & Chevalier, R. (1975). Crystal structure and interatomic distance in GaSe. *Physica Status Solidi(b)*, Vol.31, No2, pp. 469-473
- Kuroda, N. & Nishina, Y. (1980). Resonance Raman Scattering Study of Exciton and Polaron Anisotropies in InSe. *Sol. St. Commun.* Vol.34, No6, pp.481-484
- Lebedev, A.A.; Rud', V.Yu. & Rud' Yu.V. (1998). Photosensitivity of gerostructures porous silicon-layered A<sup>III</sup>B<sup>VI</sup> semiconductors. *Fizika i Tekhnika Poluprovodnikov (in Russian)*, Vol.32, No3, pp.353-355

- Malkov, M.P. (Ed.) (1985). Hand-book on physical-chemical fundamentals of cryogenics. (in Russian), Energoatomizdat, Moscow, USSR
- Martines-Pastor, J.; Segura, A. & Valdes, J.L. (1987). Electrical and photovoltaic properties of indium-tin-oxide/p-InSe/Au solar cells. *J. Appl. Phys.*, Vol.62, No4, pp.1477-1483
- Olguin, D.; Cantarero, A.; Ulrich, C. & Suassen, K. (2003). Effect of pressure on structural properties and energy band gaps of  $\gamma$ -InSe. *Physica Status Solidi (b)*, Vol.235, No2, pp.456-463
- Ormont, B.F. Structures of inorganic substances, Moscow, Gosudarstvennoje Izdatel'stvo Techniko Teoreticheskoy Literatury, 1950
- Polian, A.; Kunc, K. & Kuhn, A. (1976). Low-frequency lattice vibrations of  $\delta$ -GaSe compared to  $\epsilon$ - and  $\gamma$ -polytypes. *Solid State Communications*, Vol.19, No8, pp.1079-1082
- Shigetomi, S. & Ikari, T. (2000). Electrical and photovoltaic properties of Cu-doped  $p$ -GaSe/ $n$ -InSe heterojunction. *J. Appl. Phys.*, Vol.88, No3, pp.1520-1524
- Toyozawa, Y. (1958). Theory of line-shapes of the exciton absorption bands. *Progr. Theor. Phys.* Vol.20, No1, pp.53-81
- Zhirko, Yu.I. (1999). Investigation of the light absorption mechanisms near exciton resonance in layered crystals. N=1 state exciton absorption in InSe. *Physica Status Solidi (b)*, Vol.213, No1, pp.93-106
- Zhirko, Yu.I. (2000). Investigation of the light absorption mechanisms near exciton resonance in layered crystals. Part 2. N=1 state exciton absorption in GaSe. *Physica Status Solidi (b)*, Vol.219, No1, pp.47-61
- Zhirko, Yu. I.; Kovalyuk, Z. D.; Pyrlja, M. M. & Boledzyuk, V. B. (2007a). Application of layered InSe and GaSe crystals and powders for solid state hydrogen storage. In: *Hydrogen Materials Science and Chemistry of Carbon Nano-materials*, N.T. Veziroglu et al. (Ed.), 325-340, © 2007 Springer
- Zhirko, Yu.I.; Kovalyuk, Z.D.; Klad'ko, V.P. et al. (2007b) Investigation of hydrogen intercalation in layered crystals InSe and GaSe, *Proceedings of HTM-2007 15 International Conference "Hydrogen Economy and Hydrogen Treatment of Materials"*, Vol.2, pp. 606-610., Donetsk, Ukraine, May 21-25, 2007
- Zhirko, Yu.; Kovalyuk, Z.; Zaslonskin, A. & Boledzyuk, V. (2010). Photo and electric properties of hydrogen intercalated InSe and GaSe layered crystals, *Proceeding of Solar'10 International Conference "Nano/Molecular Photochemistry and Nanomaterials for Green Energy Development"* pp.48-49, Cairo, Egypt, February 15 -17, 2010
- Zhirko, Yu.I. (2011). Optical properties of GaSe and InSe layered crystal hydrogen intercalates. Comparative study. *Proceeding of International Symposium on Reactivity of Solids (ISRS17)*. p.14, Bordeaux, France, 27 June – 1 July, 2011

Zhirko, Yu. I.; Skubenko, N.A.; Dubinko, V. I. et al. (2012). Influence of Impurity Doping and  $\gamma$ -Irradiation on the Optical Properties of Layered GaSe Crystals. *Journal of Materials Science and Engineering B*, Vol.2, No2, pp.91-102.

IntechOpen

IntechOpen